symmetry

MDPI

Review

Radiomics and Its Feature Selection: A Review

Wenchao Zhang, Yu Guo and Qiyu Jin *

School of Mathematical Science, Inner Mongolia University, Hohhot 010020, China;
32136059@mail.imu.edu.cn (W.Z.); yuguomath@aliyun.com (Y.G.)
* Correspondence: qyjin2015@imu.edu.cn

Abstract: Medical imaging plays an indispensable role in evaluating, predicting, and monitoring a range of medical conditions. Radiomics, a specialized branch of medical imaging, utilizes quantitative features extracted from medical images to describe underlying pathologies, genetic information, and prognostic indicators. The integration of radiomics with artificial intelligence presents innovative avenues for cancer diagnosis, prognosis evaluation, and therapeutic choices. In the context of oncology, radiomics offers significant potential. Feature selection emerges as a pivotal step, enhancing the clinical utility and precision of radiomics. It achieves this by purging superfluous and unrelated features, thereby augmenting model performance and generalizability. The goal of this review is to assess the fundamental radiomics process and the progress of feature selection methods, explore their applications and challenges in cancer research, and provide theoretical and methodological support for future investigations. Through an extensive literature survey, articles pertinent to radiomics and feature selection were garnered, synthesized, and appraised. The paper provides detailed descriptions of how radiomics is applied and challenged in different cancer types and their various stages. The review also offers comparative insights into various feature selection strategies, including filtering, packing, and embedding methodologies. Conclusively, the paper broaches the limitations and prospective trajectories of radiomics.

Keywords: radiomics; feature selection; neoplasms; image processing; computer-assisted

Citation: Zhang, W.; Guo, Y.; Jin, Q. Radiomics and Its Feature Selection: A Review. *Symmetry* **2023**, *15*, 1834. https://doi.org/10.3390/sym15101834

Academic Editor: Lorentz Jäntschi

Received: 9 August 2023
Revised: 2 September 2023
Accepted: 6 September 2023
Published: 27 September 2023

1. Introduction

Cancer is the second leading cause of death worldwide. The burden of cancer continues to grow, exerting significant physical, emotional, and economic pressure on individuals, families, communities, and health systems [1]. Due to the high degree of tumor heterogeneity and recurrence rate, there is an urgent need for more effective strategies with which to detect and treat cancer. Medical imaging serves as a valuable tool in aiding the diagnosis, management, and monitoring of tumors. Techniques such as X-ray computed tomography (CT), magnetic resonance imaging (MRI), positron emission tomography (PET), and ultrasound (US) are pivotal in advancing personalized cancer diagnosis and treatment. These imaging modalities offer essential complementary information to genomic, proteomic, and metabolomic technologies, facilitating non-invasive assessments of human tissue properties [2]. Moreover, medical imaging can help identify biomarkers that predict treatment response and clinical outcomes [3]. However, the interpretation of images manually remains subjective, relying heavily on individual experience and qualitative evaluation. To enhance accuracy and reliability, identifying quantitative and reliable image biomarkers to support clinical diagnosis is essential. Radiomics, a methodology that integrates image segmentation, feature extraction, feature analysis, and data mining, has emerged as a promising approach in this domain.

Since its introduction in 2012 [4], the field of radiomics has experienced exponential growth. Although the term "radiomics" was formally coined in that year, its roots can be traced back to earlier methods in medical image texture analysis. These early techniques gradually evolved and became more sophisticated, leading to the formalization of

radiomics. This evolution encompasses the integration of more complex algorithms and machine learning models, as well as broader applications in clinical decision-making and patient management. Understanding this technological progression not only showcases the maturity of the field but also sets the stage for future research directions. A keyword search for "radiomics" on PubMed (www.ncbi.nlm.nih.gov/pubmed accessed on 28 August 2023) revealed a rising number of annual publications, as depicted in Figure 1, indicating a growing interest in radiomics. These publications primarily concentrate on the field of radiomics, encompassing the extraction and quantitative analysis of features from medical images. They cover a wide range of scientific studies, including original research, reviews, conference proceedings, and related scholarly works related to radiomics. Collectively, these publications enhance the understanding and advancement of radiomics techniques, particularly in the context of medical imaging and diagnosis.

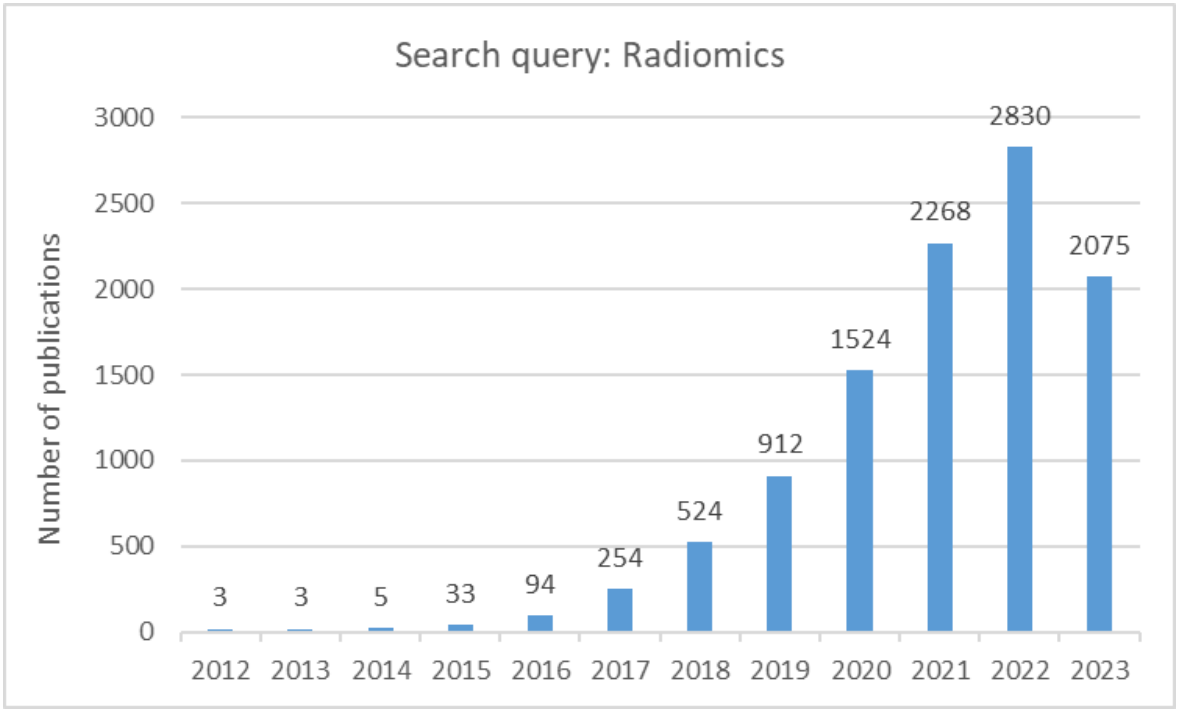

Figure 1. Number of publications related to radiation medicine in the PubMed database from 2012 to the present.

Radiomics is a fundamental medical technique used in clinical practice to aid in screening, diagnosis [5], treatment decision-making [6], and follow-up. It is a rapidly developing artificial intelligence (AI) technique in medical imaging, capable of extracting a large number of quantitative features from medical images in an objective, reproducible, and high-throughput manner. Using these extracted features, radiomics models, also known as signatures, are developed to interpret diverse clinical phenotypes, encompassing patient genotyping, treatment effectiveness, and clinical outcomes [7,8]. The core principle of radiomics is that medical images contain information relevant to the pathophysiology of certain diseases, which can be quantitatively analyzed to aid in diagnosis and treatment [9]. In oncology, the potential of radiomics lies in its capability to quantitatively evaluate intra-tumor heterogeneity, thereby unveiling phenotypes and microenvironments that might not be evident upon visual inspection [10,11]. Radiomics features, such as tumor shape, size, volume, intensity, and texture, provide information different from or complementary to clinical reports, laboratory tests, genomic, or proteomic analyses [12]. Radiomics features extracted from medical images can be categorized into two types: hand-crafted features obtained through traditional algorithms (such as intensity, shape, texture, and wavelets) and features generated through deep learning (DL) algorithms. Hand-crafted features

offer specific information about the regions of interest (ROIs) within medical images, such as tumors or organs, and can be correlated with additional data sources, including clinical, treatment, or genomic data [13]. Meanwhile, DL features are acquired through the training of DL networks. In recent years, DL has gained popularity, primarily due to the exceptional performance of convolutional neural networks (CNNs) in tasks such as image classification and recognition in the field of medical imaging [14,15]. This trend has opened up new opportunities for research in radiomics. CNNs enable the extraction of DL features that capture intra-tumor heterogeneity, facilitating direct information extraction from medical images and providing a more accurate description of tumor characteristics compared to manually designed radiomics features [16,17]. The rationale behind this trend is well-founded, as CNNs have consistently demonstrated remarkable performance in medical imaging, offering strong support for their application in radiomics research. The advantage of DL is its ability to bypass the need for extensive data processing, making it more efficient. However, a notable limitation of DL is its "black box" nature; the resulting models and features often lack interpretability, which can impede their direct applicability in clinical scenarios. Additionally, DL methods are efficient when applied to large datasets. However, the sample size, especially in rare diseases, is not always sufficient to fully utilize these architectures [18]. Therefore, transfer learning is proposed to bridge this gap. Transfer learning involves using pre-trained models from images in other domains and fine-tuning the parameters of the model on the target dataset to make it applicable to the target task [19,20]. This process is widely used in the field of medical image analysis [21]. By combining both hand-crafted features and DL features with other patient data, such as pathology results, clinical records, and genomic data, more precise and robust predictive models of clinical outcomes can be developed.

Radiomics has gained significant attention in recent years for its ability to identify tumor genotypes and pathological imaging biomarkers, which have clinical potential [22,23]. Studies have indicated that radiomics has the potential to improve or surpass existing tumor diagnosis methods, as it can effectively evaluate genomic features [24,25], tumor subtypes [26–28], and lymph node metastasis [29–32] in various cancers. Radiomics has demonstrated the ability to predict the prognosis of various malignancies, including colorectal cancer [33–38], gastric cancer [39–44], cervical cancer [31,45–48], pancreatic cancer [49–51], nasopharyngeal cancer [52–57], breast cancer [58–62], and lung cancer [63–68]. To conduct a comprehensive literature review, we employed the PubMed search engine in combination with an online literature tracking tool named Stork (https://www.storkapp.me/ accessed on 8 March 2023). Stork serves as a researcher's personalized scientific information assistant, designed to seamlessly provide the most recently published scientific literature based on the researcher's preferences. This enables real-time engagement with the latest advancements. Additionally, Stork provides a wide range of advanced features. It dynamically acquires and analyzes a significant amount of scientific literature, then presents statistical insights using informative charts and graphs, significantly enhancing user productivity. In our study, we utilized this invaluable tool in conjunction with the PubMed search engine to curate relevant articles in the field of radiomics. Our search included relevant articles up to 8 March 2023, covering a broad spectrum of radiomics research, with a notable focus on lung and breast cancers (Figure 2).

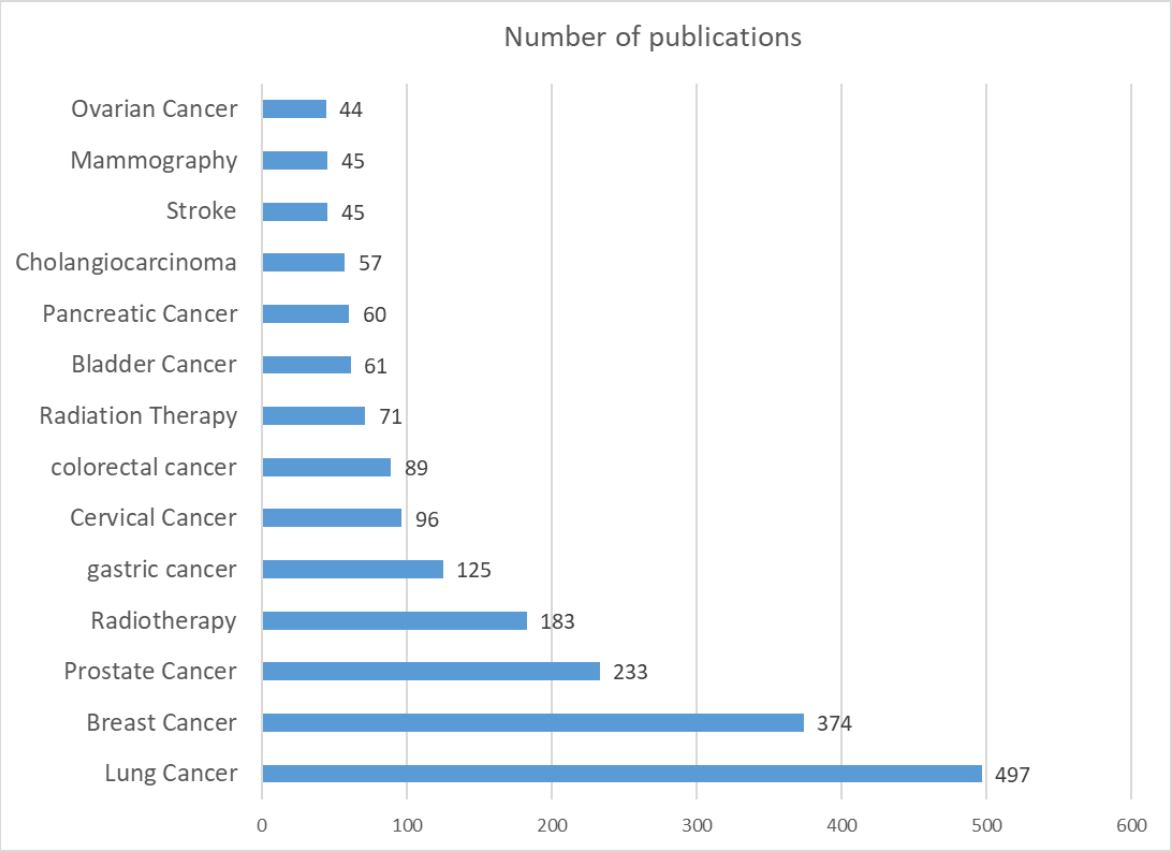

Figure 2. Radiomics techniques have been applied to variety of diseases.

The radiomics workflow comprises five distinct stages, each presenting specific challenges that researchers aim to overcome. Thee are as follows. Image acquisition and pre-processing: Ensuring the quality and consistency of the images before analysis. Image segmentation: Defining the boundaries of the ROIs using various methods, including manual, semi-automatic, and automatic methods. Feature extraction and selection: Extracting quantitative characteristics from the tumor area using specialized open-source or internally created software, followed by selecting a relevant subset of features. This step aims to reduce the number of predictors while retaining essential data for the study results. Model creation and evaluation: Building models involves various techniques, ranging from simple linear regression to complex machine learning methods such as random forests (RF), support vector machines, and neural networks. The evaluation of predictive models typically considers identification, calibration, and potential clinical value. Clinical application: Radiomics assists clinicians in making supplementary diagnoses and in guiding subsequent treatment decisions. In this review, we begin with an overview of each step in the radiomics workflow (Section 2). Subsequently, we comprehensively examine feature selection, which is one of the vital steps in radiomics studies, in Section 3. This section aims to aid researchers in constructing more effective radiomics models by offering insights into various feature selection methods. Section 4 discusses conventional and DL-based radiomics, highlighting the pros and cons of three feature selection methods commonly used in radiomics studies. In addition, it discusses the challenges facing radiomics and introduces the development of radiomics in a new perspective. Lastly, Section 5 presents the conclusions.

2. Radiomics Workflow

The radiomics workflow is divided into five key stages, each with its own specific challenges. Radiomics employs various feature extraction algorithms to transform imaging data from the ROIs into either first-order or higher-order features. This process aims to

enhance clinical diagnostic accuracy and prognostic/predictive value by exploring and evaluating data relationships. Figure 3 depicts the fundamental radiomics process.

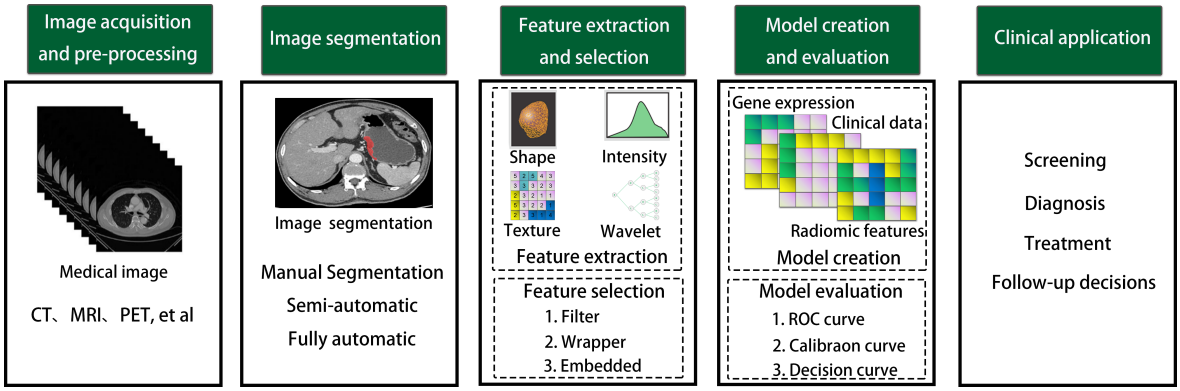

Figure 3. Radiomics Workflow.

2.1. Image Acquisition and Pre-Processing

In radiomics, the workflow consists of five critical stages, each presenting unique challenges. The initial stage involves image acquisition using various modalities such as CT, MRI, PET, and US. One of the primary obstacles at this stage is the high variability in image acquisition procedures across different medical centers. This variability can compromise the reproducibility of quantitative features and, by extension, the external validity of radiomics models [69,70]. Given the complexities involved in image normalization, radiomics models must undergo internal and external testing in multiple validation cohorts to ensure accuracy. Therefore, one of the major challenges in radiomics is to reduce the influence of the imaging protocol on radiomics features. Many studies use multicenter data to assess the robustness of radiomics models under different image parameters [71–73].

Additionally, post-image acquisition pre-processing can mitigate the impact of certain image acquisition parameters on the model. The future of pre-processing depends on establishing standardized imaging protocols and image preprocessing procedures, including pixel spacing, gray intensity, and gray-level histogram bins. Nevertheless, the substantial variations among different imaging techniques necessitate additional quality control measures to ensure study reproducibility. Various initiatives have been proposed to establish acquisition and reconstruction criteria, aiming to advance quantitative imaging and ensure reliability. For instance, the Radiological Society of North America and the National Institute for Biomedical Imaging and Bioengineering have supported the Quantitative Imaging Biomarkers Alliance (QIBA) [74], and the European Society of Radiology has established the European Imaging Biomarkers Alliance subcommittee (EIBALL) [75].

2.2. Image Segmentation

After collecting a robust image dataset from the target patient cohort, the next crucial step is to accurately segment ROIs or Volumes of Interest (VOIs). Radiomics features are notably influenced not only by image acquisition but also by the variability in ROIs delineation. Precise ROIs segmentation is a pivotal step in radiomics investigations as it significantly affects the derived radiomics features. Segmentation methods include manual, semi-automatic, and fully automatic approaches. Typically, expert clinicians or researchers perform manual ROIs delineation, which serves as the benchmark. However, manual segmentation is resource-intensive and relies on trained practitioners to reduce inter-operator inconsistencies. In cases where lesion boundaries are unclear or multiple focal lesions are present, multiple manual segmentations may be needed in order to ensure accuracy and reproducibility. Despite being time-intensive and susceptible to bias, evaluating the reproducibility of reported features among different observers is essential. Radiomics attributes that lack repeatability should be discarded [76]. Feature consistency within and among observers can be quantified using the Intraclass Correlation Coefficient (ICC) [77].

In summary, following dataset collection, precise segmentation becomes the focal point, as it plays a significant role in the consistency and reproducibility of radiomics features.

Many studies indicate that employing automatic or semi-automatic segmentation techniques can mitigate human errors, enhancing efficiency. There are numerous software programs and segmentation algorithms available for performing semi-automatic and fully automatic segmentation of radiomics images. Examples of segmentation software widely used in medical research include 3D Slicer [78], ITK-SNAP [79], ImageJ [80], and MITK/3DMed [81,82]. Semi-automatic or fully automatic segmentation is appealing because it provides a more reproducible and efficient approach to observing robust features within a given ROIs [83]. While automated methods for medical image segmentation are becoming more accurate, they still depend on manual outlining as the gold standard. There is a growing belief that optimal and reliable segmentation can be achieved through a combination of computer-aided edge detection and manual refinement [84].

Computer-aided inspection systems commonly employ a variety of segmentation techniques, including active contour, level-set, area-based, and graph-based methods [85,86]. Parametric techniques, such as active contour and level-set models, require appropriate initialization and may have limitations when handling uncertain shapes or unknown ROIs locations. Region-based methods, which rely on pixel intensity homogeneity, may encounter challenges in scenarios involving complex anatomical structures or undefined ROIs. In contrast, graph-based methods effectively capture pixel interactions [87], making them suitable for handling complex anatomical structures, albeit with a potential increase in computational load.

Conversely, DL has emerged as a powerful paradigm for medical image segmentation, consistently achieving remarkable results across various applications in medical imaging [88]. Unlike traditional approaches that depend on hand-crafted features and algorithms, DL techniques learn directly from data, capturing intricate patterns and representations that are challenging to express through explicit rules. One key advantage of DL-based segmentation is its adaptability to a wide range of medical imaging tasks.

Prominent DL architectures for medical image segmentation include Unet [89], ST-Unet [90], Unet++ [91], Eres-UNet++ [92], CE-Net [93], and PIPO-FAN [94]. These foundational frameworks excel in segmenting structures and anomalies within medical images. Nevertheless, DL models are specific to particular tasks and necessitate customized training. Similar to the selection of different methods for different contexts, DL networks are specialized and may not perform effectively beyond their trained domain. In the field of medical imaging, misapplication of models can have serious consequences. Therefore, DL-based medical image segmentation systems require a well-considered combination of methodologies capable of adapting to diverse conditions. By understanding the strengths and limitations of models and incorporating them intelligently, medical professionals and researchers can effectively utilize DL for precise image segmentation in scenarios with intricate anatomies or undefined ROIs.

2.3. Feature Extraction and Feature Selection

Following tumor area segmentation, the subsequent critical step involves extracting features from the image. Automated radiomics feature extraction can be accomplished using various open-source software tools, including LIFEx (https://www.lifexsoft.org/index.php accessed on 8 August 2023), MITK (http://www.mitk.org/wiki/MITK accessed on 8 August 2023), CERR (https://github.com/cerr/CERR accessed on 8 August 2023), and others. Alternatively, open-source software packages such as pyRadiomics [95] can be used for feature extraction. In the realm of radiomics, data-driven methodologies eliminate prior assumptions concerning the clinical significance of particular features. Utilizing advanced open-source software tools, these algorithms autonomously identify, compute, and extract features, thereby revealing novel patterns pivotal for both diagnosis and prognosis. Importantly, the choice of software for feature extraction can introduce variability, potentially affecting the consistency and reliability of the resulting data.

In response to this challenge, Zwanenburg et al. introduced the Image Biomarker Standardization Initiative (IBSI) [96], which consists of a standardized set of 169 features. This initiative facilitates the validation and calibration of various radiomics software tools and addresses the variations and inconsistencies in radiological feature extraction methods employed across different studies and clinical settings. Consequently, it enhances the reliability and comparability of radiological image features and provides guidance for future research.

To ensure the reproducibility of radiomics-based models, it is crucial to extract radiomics features from pre-processed imaging data that have been optimized to reduce inconsistencies. Image normalization is a vital technique that ensures consistent distribution of different images within a similar value range. It is necessary for facilitating image comparisons and consistent analysis. Resampling images to the same size facilitates easier comparison and analysis. These strategies mitigate discrepancies caused by different acquisition devices, parameters, and factors. Radiomics features fall into three primary categories:–first-order statistical, shape-based, and texture features—as depicted in Table 1. First-order statistical features analyze the distribution of individual voxel values without considering spatial relationships. They reflect the symmetry, homogeneity, and local intensity distribution variations of the measured voxels.

Table 1. Commonly extracted first-order, shape-based, and texture features.

First-order features	**Shape-based features**	**Texture features**				
		Gray Level Co-occurrence Matrix(GLCM)	Gray Level Size Zone Matrix(GLSZM)	Gray Level Dependence Matrix(GLDM)	Gray Level Run Length Matrix(GLRLM)	Neighboring Gray Tone Difference Matrix(NGTDM)
Energy	Mesh Volume	Autocorrelation	Small Area Emphasis	Small Dependence Emphasis	Short Run Emphasis	Coarseness
Total Energy	Voxel Volume	Joint Average	Large Area Emphasis	Large Dependence Emphasis	Long Run Emphasis	Contrast
Entropy	Surface Area	Cluster Prominence	Gray Level Non-Uniformity	Gray Level Non-Uniformity	Gray Level Non-Uniformity	Busyness
Minimum	Surface Area to Volume ratio	Cluster Shade	Gray Level Non-Uniformity Normalized	Dependence Non-Uniformity	Gray Level Non-Uniformity Normalized	Complexity
10th percentile	Sphericity	Cluster Tendency	Size-Zone Non-Uniformity	Dependence Non-Uniformity Normalized	Run Length Non-Uniformity	Strength
90th percentile	Maximum 3D diameter	Correlation	Size-Zone Non-Uniformity Normalized	Gray Level Variance	Run Length Non-Uniformity Normalized	
Maximum	Maximum 2D diameter (Slice)	Difference Average	Zone Percentage	Dependence Variance	Run Percentage	
Mean	Maximum 2D diameter (Column)	Difference Entropy	Zone Variance	Dependence Entropy	Gray Level Variance	
Median	Maximum 2D diameter(Row)	Difference Variance	Zone Entropy	Low Gray Level Emphasis	Run Variance	
Interquartile Range	Major Axis Length	Joint Energy	Low Gray Level Zone Emphasis	High Gray Level Emphasis	Run Entropy	
Range	Minor Axis Length	Joint Entropy	High Gray Level Zone Emphasis	Small Dependence Low Gray Level Emphasis	Low Gray Level Run Emphasis	
Mean Absolute Deviation	Least Axis Length	Informational Measure of Correlation	Small Area Low Gray Level Emphasis	Small Dependence High Gray Level Emphasis	High Gray Level Run Emphasis	
Robust Mean Absolute Deviation	Elongation	Inverse Difference Moment	Small Area High Gray Level Emphasis	Large Dependence Low Gray Level Emphasis	Short Run Low Gray Level Emphasis	
Root Mean Squared	Flatness	Maximal Correlation Coefficient	Large Area Low Gray Level Emphasis	Large Dependence High Gray Level Emphasis	Short Run High Gray Level Emphasis	
Skewness		Inverse Difference Moment Normalized	Large Area High Gray Level Emphasis		Long Run Low Gray Level Emphasis	
Kurtosis		Inverse Difference			Long Run High Gray Level Emphasis	
Variance		Inverse Difference Normalized				
Uniformity		Invers Variance				
		Maximum Probability				
		Sum Average				
		Sum Entropy				
		Sum of Squares				

These include median, mean, minimum, maximum, standard deviation, skewness, kurtosis, and more. Shape features describe the shape of the traced ROI and its geometric properties, including volume, maximum diameter along different orthogonal directions, maximum surface, tumor compactness, and sphericity. For instance, the surface-to-volume ratio of a spiculated tumor will exhibit higher values compared to that of a round tumor with similar volume [97]. Second-order and higher-order texture features can discern or gauge spatial variations in voxel intensity levels by evaluating the spatial dispersion among voxels [98]. Textural features can be categorized into several groups, as depicted in Figure 4.

1. The Gray Level Co-occurrence Matrix (GLCM) represents the probability of a voxel value occurring at a specific direction and distance [99,100];
2. The Gray Level Run Length Matrix (GLRLM) describes the length of consecutive voxels with the same gray level in a specified direction [101,102];
3. The Gray Level Size Zone Matrix (GLSZM) segments an image into regions with contiguous voxel values [103];
4. The Neighboring Gray Tone Difference Matrix (NGTDM) quantifies the gray value of a voxel by considering the difference between its average gray value and the gray value within a certain distance of the neighborhood [104];
5. The Gray Level Dependence Matrix (GLDM) calculates the difference between adjacent voxels based on their values [105].

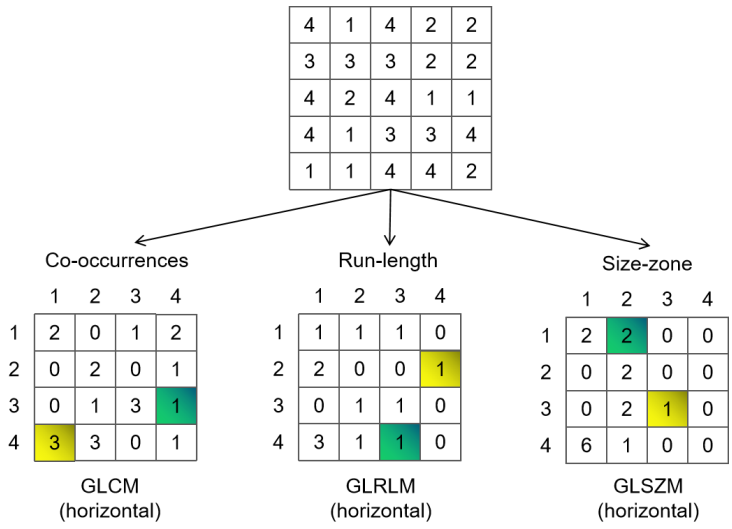

Figure 4. Examples of specific matrices that allocate information about the spatial distribution of pixel values in the image.

Additionally, DL offers a meaningful approach to extract deep features. DL models consist of trainable nonlinear operations, referred to as layers, that transform input data into representations for effective pattern recognition. The addition of more layers to the model progressively abstracts the input data, resulting in a deep-feature representation [106]. An illustration of utilizing a DL network to extract features of occult peritoneal metastases from gastric cancer [107] is presented in Figure 5. DL algorithms possess the ability to automatically learn phenotypic features, exhibiting powerful characterization capabilities without requiring predefined characteristics or human intervention [108,109]. It is important to acknowledge that not all extracted features are beneficial for modeling. Therefore, data cleaning plays a crucial role in the process, encompassing error identification and correction in data files, validation of data consistency, and handling invalid and missing values.

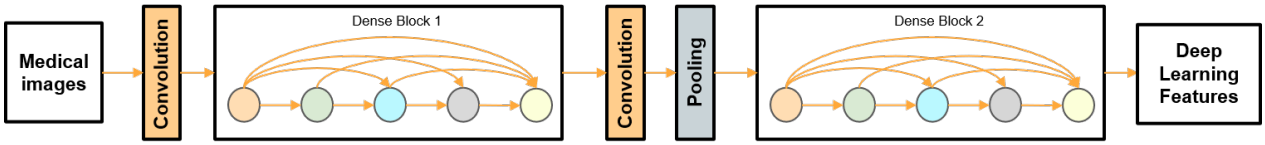

Figure 5. DL network to extract radiomics features.

Following feature extraction, it becomes essential to choose a subset of these features tailored to a specific disease process or research question. Radiomics features can be categorized based on their relevance to machine learning and their potential to enhance the performance of learning algorithms. The first category comprises relevant features that significantly benefit machine learning and enhance the efficiency of learning algorithms. The second category refers to irrelevant features that do not aid the algorithm and do not contribute to its learning process. Lastly, the third category consists of "redundant features", which can be inferred from other available information and do not offer new insights to the learning algorithm.

Feature selection is a crucial step in the radiomics workflow, aimed at eliminating irrelevant or redundant features while retaining those that are relevant and useful. This process helps reduce the dimensionality of features, enabling machine learning models to learn more efficiently and reducing the risk of overfitting. The goal of feature selection is to identify a smaller subset of features that are most relevant and predictive for the specific task at hand. Additionally, feature dimensionality reduction involves reducing the dimensionality of the correlation feature matrix, which further enhances the efficiency and effectiveness of the radiomics analysis.

2.4. Model Creation and Evaluation

After selecting the radiomics features, they can be used in various models, such as diagnostic, prognostic, or predictive models [76]. Machine learning has become a prevalent method for radiomics-based predictions, owing to the rapid growth in high-dimensional data availability in recent years. The core concept of machine learning involves training models on input-output examples, allowing the system to learn desired relationships autonomously, without extensive human programming. To achieve this, numerous machine learning classifiers have been developed, employing a diverse range of candidate algorithms [110–114]. These classifiers aim to achieve optimal performance through repeated iterations of training and testing. Several popular classifiers include Extreme Gradient Boosting, RF, Naive Bayes, and Support Vector Machine (SVM). In radiomics studies, evaluating the predictive accuracy of multiple classifiers, feature selection methods, and their combinations is crucial for selecting the most suitable machine learning classifier for a given research problem or dataset [115]. Overfitting and underfitting can impact both statistical learning and machine learning models, resulting in unstable models that lack generalization ability. Employing strategies such as cross-validation, external validation, and multicenter validation during model training can lead to more stable models.

The receiver operating characteristic curve (ROC curve) is a common method used to evaluate the predictive accuracy of radiomics-based models. Moreover, other metrics, such as the area under the ROC curve (AUC), accuracy, precision, recall, and F1 score, are commonly used to assess the performance of the model. Independent validation, including external validation using datasets from different institutions, is a critical step in radiomics studies. Most existing radiomics studies are constrained by small sample sizes from a single institution, limiting the conclusions that can be drawn from them. To overcome this limitation, future radiomics studies should undergo validation and refinement through multiple large-scale, randomized controlled clinical trials. This approach will enhance the accuracy, reliability, and effectiveness of radiomics-based models.

2.5. Clinical Application

Radiomics has broad applications in medical research involving imaging techniques. It aids clinicians in reducing image analysis subjectivity, supporting supplementary diagnosis, and guiding appropriate follow-up treatment. Park et al. performed a meta-analysis to assess the scientific quality of radiomics studies using the Radiomics Quality Score (RQS) and Transparent Reporting of a multivariable prediction model for Individual Prognosis Or Diagnosis (TRIPOD). The analysis showed that 91% of radiomics studies are focused on oncology, and 81% of these studies are utilized for diagnostic purposes [116].

3. Feature Selection Method

Radiomics entails the development of dependable predictive biomarkers, often referred to as features in the context of machine learning. This section offers a comprehensive introduction to the process of feature selection in radiomics and the associated methodology. In the realm of radiomics, we meticulously extract numerous features from medical images. Nonetheless, it is essential to recognize that certain features may not be relevant to the specific outcome of interest. It is worth noting, however, that an excessive number of features can potentially result in overfitting, which may compromise the model's ability to make accurate predictions. Importantly, the presence of highly correlated or collinear features can have a detrimental impact on machine learning models. This stems from the foundational assumption of most models, which assumes the independence of input features. Faced with substantial correlation or collinearity, models may overly depend on these interconnected features, thereby sidelining other relevant information. This situation inevitably results in a reduction in the model's ability to effectively generalize to new data. The correlations between features that the model learns from the training data may not apply to new datasets. To enhance the model's resilience and generalization capabilities, it is often necessary to prune or consolidate closely correlated features during the training phase. This careful curation aims to reduce the model's tendency to overfit to a specific dataset, ultimately improving its performance when confronted with previously unobserved data [117–119].

Feature selection is a vital component of radiomics, as it reduces data complexity by eliminating redundant and irrelevant features, thus enhancing model performance. Various feature selection methods have been proposed, and attempts have been made to compare their performance using data from different sources. However, there is no clear consensus on the best feature selection method for radiomics [120]. A wide range of feature selection methods exists; however, the absence of a uniform reference standard for removing redundant and irrelevant features may introduce a certain level of "arbitrariness" in the feature selection process. A strong understanding of feature selection techniques is essential when developing machine learning models; without it, creating effective and useful models can be challenging.

3.1. The Feature Selection Framework

The feature subset obtained through feature selection should be as small as possible while effectively identifying the target. Additionally, it should ideally improve the accuracy of the prediction model and not reduce it. Furthermore, the class distribution of the resulting subset should closely resemble that of the original data. Dash et al. [121] proposed a search-based framework, as depicted in Figure 6A, for achieving this goal of feature selection. The framework outlines four basic steps of feature selection: candidate feature subset generation (search strategy), subset evaluation, stopping criterion, and result validation. The search strategy involves searching for feature subsets and evaluating them for further analysis. Subset evaluation involves assessing the quality of a subset of features. The stopping criterion is met when the evaluation function reaches a specific benchmark. Finally, result validation involves assessing the accuracy of the selected feature subset on the validation dataset. The search strategy and subset evaluation are vital components of any feature

selection method. The process of generating and evaluating subsets is iterated until the desired results are achieved.

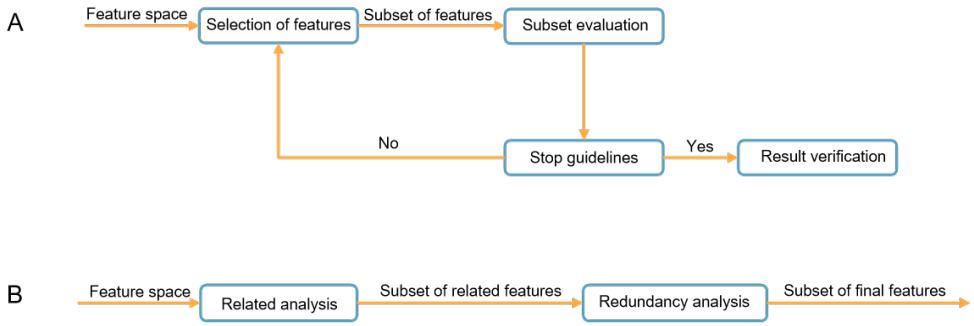

Figure 6. Image (**A**) indicates search-based framework; image (**B**) indicates relevance-based framework.

Subset search in a search-based framework can be time-consuming, especially with large datasets. Yu et al. [122] proposed an efficient feature selection framework based on correlation and redundancy analysis (Figure 6B). It avoids subset search and quickly identifies the optimal subset. The original feature set can be divided into four subsets: uncorrelated, redundant, weakly correlated but non-redundant, and strongly correlated features [123]. The relevance-based framework identifies the most pertinent features by calculating their redundancy and relevance based on a specific metric. Feature selection algorithms under this framework include Minimum Redundancy Maximum Relevance (mRMR) [124], Correlation-based Feature Selection (CFS) [125], and Fast Correlation-Based Filter solution (FCBF) [122,126].

3.2. Classification of Feature Selection

Classification of feature selection methods can be based on their relationship with the learning algorithm, determining whether they are independent or dependent. Feature selection can be categorized into three distinct categories: filter (Figure 7A), wrapper (Figure 7B), and embedded (Figure 7C) [127,128].

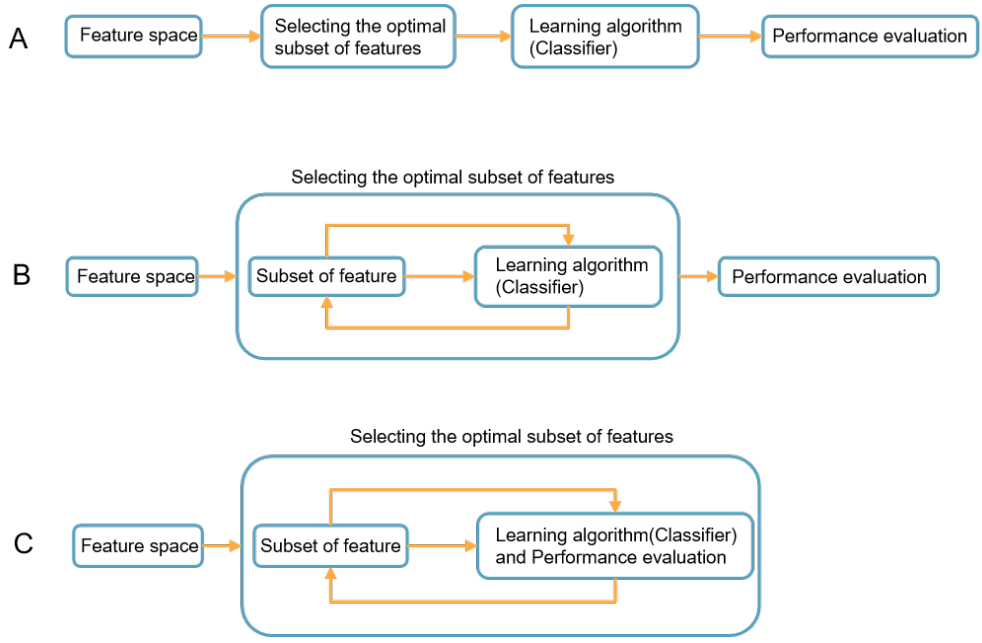

Figure 7. Subfigure (**A**) depicts the filter method, while Subfigure (**B**) illustrates the wrapper method, and Subfigure (**C**) shows the embedded method.

The filter method relies on the intrinsic characteristics of the analyzed data and evaluates features independently of any learning algorithms. The method utilizes metric matrices obtained directly from the data, eliminating the need for feedback from learning algorithms to adjust feature selection. Feature selection is determined by the features' dispersion or relevance, and unimportant ones are filtered out using a threshold or predetermined number. The growing availability of high-dimensional big data has led to increased interest in filter models, which are not biased towards a specific learner model, so its structure is always simple. Some common filter methods are listed in Table 2.

Table 2. Frequently used filtered feature selection methods.

Filter Methods	Selection Rules
Missing Percentage	Features with a disproportionate share of missing samples and difficult to fill were removed.
Variance	Features with variance close to or equal to 0 were excluded.
Frequency	Features that are excessively concentrated in one category of values are removed.
Pearson Correlation Coefficient [129,130]	Features with correlation coefficients close to or equal to 0 were excluded.
Spearman's Rank Correlation Coefficient [131,132]	Features with correlation coefficients close to or equal to 0 were excluded.
Kendall's tau Rank Correlation Coefficient	Features with correlation coefficients close to or equal to 0 were excluded.
Analysis of variance (ANOVA) [133,134]	Exclude features with too low an F-value, or exclude features with a p-value < 0.05.
Chi-squared Test [135,136]	Features with too low a chi-squared value were excluded, or features with a p-value < 0.05 were excluded.
Mutual Information [137,138]	Features with mutual information close to or equal to 0 were removed.
mRMR [124]	The features with the minimum correlation and maximum redundancy were removed.
Fisher Score [139]	Features with large intraclass distances and small interclass distances were excluded.

The wrapper method distinguishes itself from the filter method by utilizing a predetermined learning algorithm to evaluate and identify a subset of features. Instead of relying on independent metrics, the wrapper method considers the feature selection algorithm as part of the learning process and utilizes the classification performance as an evaluation criterion for feature importance. Evaluating a subset of features with a machine learning algorithm enables the detection of interactions between features, leading to the selection of an optimal feature subset for the model. The wrapper method involves both feature subset search and evaluation metrics. The former generates candidate feature subsets, while the latter trains and evaluates a model with each feature subset using a validation set to identify the optimal one. Subset search is a vital step in wrapper methods, and it employs three types of search methods as depicted in Table 3. Common examples of wrapper methods are Recursive Feature Elimination (RFE) [140] and RF.

Table 3. Feature subset search algorithms.

Classification of Search Strategies (Subset Generation Process)	Algorithm Features	Subset Search Algorithm
Complete search	Iterate through all possible combinations of feature subsets, then select the feature subset with the best model score.	Breadth First Search [141] Best First Search [142]
Heuristic search	The search is evaluated for each location searched, the best position is obtained, and the search is carried out from this position until the target is reached.	Sequential Forward Selection (SFS) [143,144] Sequential Backward Selection (SBS) [145] Bidirectional Search (BDS) [146] Plus-L Minus-R Selection (LRS) [147] Sequential Floating Selection (SFS) [148] Decision Tree Method (DTM) [149]
Random search	A random subset of features is generated and then these feature subsets are given an evaluation.	Random Generation plus Sequential Selection (RGSS) [146] Simulated Annealing (SA) [150] Genetic Algorithms (GA) [151]

Filter methods exhibit computational efficiency, but they do not account for the bias of the learning algorithm. Conversely, wrapper methods offer a more accurate prediction estimate by considering the learning algorithm's bias, yet they may incur computational expenses. Embedded methods merge the benefits of filter and wrapper methods by integrating feature selection into the model construction process. Embedded methods effectively utilize both filter and wrapper methods: (1) they are significantly less computationally intensive than wrapper methods as they do not necessitate multiple runs of the learning model to evaluate features; and (2) they interact with the learning model. The key distinction between the wrapper and embedded methods lies in the process of utilizing candidate features. The wrapper method initially trains the learning model using candidate features and then evaluates the features through feature selection using the learning model. In contrast, the embedded method selects features during feature model construction without the need for further evaluation through feature selection. Examples of embedded methods are Least Absolute Shrinkage and Selection Operator (LASSO) [152] and Gradient Boosted Decision Trees (GBDT) [153]. A summary of the advantages and disadvantages of the filter, wrapper, and embedded models is presented in Table 4.

Table 4. Advantages and disadvantages of filters, wrappers and embedded methods.

Category	Advantage	Disadvantages
Filter	More efficient calculation Effectively avoid over-fitting Independent of the learning algorithms	Ignores interaction with the learning algorithms Weakeed learer fitting ability
Wrapper	Simple Interacts with the learning algorithms Models feature dependencies	Risk of overfitting Learning algorithms-dependent selection A large number of calculations
Embedded	Interacts with the learning algorithms Less complexity than Wrapper More efficient calculation	Learning algorithms-dependent selection Increases the model training burden

Radiomics studies often employ five primary feature selection methods. These are as follows:

1. Distribution Analysis: The Mann–Whitney U-test measures the difference in the distribution of each feature within the positive and negative sample groups. The formula for U_i is as follows:

$$U_i = R_i - \frac{n_i(n_i+1)}{2}, \tag{1}$$

where i represents the positive or negative group, n_i is the data size of group i, and R_i is the sum of the ranks in group i. Smaller values of U_i are consulted in significant tables to derive a p-value. A smaller p-value indicates that the corresponding feature can effectively distinguish positive and negative samples. Anderson–Darling (AD) test is also a widely used method. The AD test is primarily used for testing whether data conform to a specific distribution, such as the normal or exponential distribution. However, it can also be employed for feature selection in machine learning. When used for feature selection, the goal of the AD test is to assess how effectively the distribution of a given feature distinguishes different categories or outcomes within a dataset. A feature that produces significantly different distributions may be a good candidate for inclusion in a machine learning model. The mathematical formula for the Anderson–Darling test is as follows:

$$A^2 = -n - \frac{1}{n}\sum_{i=1}^{n}(2i-1)[\ln(F(x_i)) + \ln(1 - F(x_{n+1-i}))], \tag{2}$$

where n is the sample size, x_i represents the i-th ordered observation, and $F(x_i)$ is the theoretical cumulative distribution function value for x_i . Higher values of A^2 indicate a worse fit between the sample data and the chosen distribution. Critical values of A^2 and corresponding p-values are commonly looked up in a distribution table or calculated using software. A smaller p-value, typically below a significance level of 0.05 or 0.01, indicates the rejection of the null hypothesis, suggesting that the data do not come from the specified distribution. A small p-value suggests that the feature can effectively differentiate between different categories.
2. Decorrelation: The Pearson linear correlation coefficient calculates the correlation between each pair of features:

$$r = \frac{\sum_{n=1}^{N}\left(x_n^i - \overline{x^i}\right)\left(x_n^j - \overline{x^j}\right)}{\sqrt{\sum_{n=1}^{N}\left(x_n^i - \overline{x^i}\right)^2}\sqrt{\sum_{n=1}^{N}\left(x_n^j - \overline{x^j}\right)^2}}, \tag{3}$$

where x^i and x^j represent two different features of the patients in the training cohort, and N is the data size of the training cohort.
3. Minimum Redundancy Maximum Relevance (mRMR): The mRMR method selects features that are distant from each other while still being highly correlated with the predicted labels. The method is based on mutual information, defined as follows:

$$I(x;y) = \int\int p(x,y)\log\frac{p(x,y)}{p(x)p(y)}p(x,y). \tag{4}$$

Assuming a total of X features, $m-1$ of them are selected to create the feature set $S_{(m-1)}$. The m-th feature can be selected through a stepwise optimization process using the objective function.

$$\max_{x^j \in X - S_{m-1}}\left[I\left(x^j;y\right) - \frac{1}{m-1}\sum_{x^i \in X - S_{m-1}} I\left(x^j;x^i\right)\right] \tag{5}$$

In the equation, y represents the classification variables of the samples in the training cohort, while x^i and x^j represent distinct features of the patients in the same training cohort.

4. The Least Absolute Shrinkage and Selection Operator (LASSO) is a linear model that incorporates an L_1-norm regularization to encourage sparse variable coefficients. It selects features with non-zero coefficients to form the final potential descriptor group for each specific task. The optimization objective for LASSO is represented as follows:

$$\min_{\omega} \sum_{n=1}^{N} \left(y_n - \omega^T x_n \right)^2 + \lambda |\omega|_1. \tag{6}$$

Here, x_n represents the feature vector of the n-th patient, y_n is the classification variable, ω denotes the weight vector of the linear model, and $\lambda > 0$ is the normalization parameter [154].

It is important to note that once feature selection is completed, the model is trained. However, if the feature matrix becomes too large after the selection process, it can lead to prolonged computation times and extended training durations, potentially requiring more powerful hardware. Therefore, it becomes essential to reduce the dimensionality of the feature matrix, a process known as feature dimensionality reduction.

Feature dimensionality reduction can enhance the performance of radiomics models [155]. Feature selection and dimensionality reduction serve a common purpose: addressing high dimensionality in data processing, where the number of features in a sample tends to increase linearly with the amount of data to be processed. Feature selection and dimensionality reduction involve substituting high-dimensional features with more suitable and representative ones through specific algorithms. Nevertheless, these two methods differ in their approaches. Dimensionality reduction is mainly accomplished by analyzing the relationships between features, for example, by combining different features to create new ones, thereby altering the original feature space. In contrast, feature selection involves choosing a subset of the original feature dataset without altering the original feature space, and it operates based on an inclusion relationship. Common dimensionality reduction techniques comprise the L_1 -based penalty model (e.g., LASSO), as well as principal component analysis (PCA) [156,157] and linear discriminant analysis (LDA) [158,159], all of which map the original data to a lower-dimensional sample space.

Feature selection serves the purpose of assisting in the construction of radiomics models for disease diagnosis and prediction. The study conducted by Huang et al. [160] stands as an exemplary demonstration of effective feature selection in radiomics research, offering valuable insights into the selection and application of radiomics features in specific cancer cases. In this study, radiomics was applied to early-stage non-small-cell lung cancer (NSCLC) cases, aiming to construct a robust model for predicting disease-free survival (DFS). Feature selection was a vital step, meticulously executed to identify the most informative radiomics features associated with DFS. The study assembled a cohort consisting of early-stage NSCLC patients and created an extensive dataset encompassing CT and PET images. Using specialized image analysis software, a diverse range of radiomics features, encompassing shape, texture, and intensity attributes, were extracted from the images of each patient. The research employed the following strategies for feature selection: Initially, an exploration phase involved calculating Pearson correlation coefficients to assess the relationship between individual radiomic features and DFS. This analysis offered insights into the extent of correlation between features and DFS. Subsequently, further refinement of the feature set was accomplished through LASSO regression, which, owing to its capacity to induce sparsity in coefficients, identified the most predictive radiomics features. After feature selection, a predictive model for estimating early-stage NSCLC patient DFS was constructed. Rigorous validation procedures, including cross-validation, were employed to assess the performance of the model. The thorough application of the feature selection process ultimately defined a distinctive set of radiomics features known as the "radiomics signature". This signature succinctly summarized radiomic features strongly correlated

with the prediction of DFS in early-stage NSCLC patients. Significantly, during model validation, the "radiomics signature" exhibited strong predictive performance. Through the integration of correlation analysis and LASSO regression, researchers successfully identified a subset of radiomics features possessing significant prognostic value. The established radiomics signature has substantial potential for improving prognostic accuracy, consequently enhancing clinical decision-making and patient management capabilities in early-stage NSCLC cases.

4. Discussion

Traditional radiomics involves extracting numerous hand-crafted features from ROIs and then performing feature selection to identify those relevant to a specific task. This method, while somewhat effective in various applications, is criticized for introducing human bias into the feature computation process. In contrast, DL-based radiomics directly extracts features from images, eliminating the need for intermediate operations in feature computation and reducing the risk of information loss or additional errors. Various deep network architectures can be designed to meet specific requirements. The hierarchical structure of deep neural networks facilitates the discovery of deeper and higher-level features, in contrast to the shallow features typically identified in traditional machine learning algorithms [161]. Previous studies have shown that DL methods demonstrate high accuracy and offer promising clinical prospects [41,162,163]. However, Zhang et al. [164] have highlighted that black-box algorithms may potentially hinder the reliability of their clinical applicability.

Radiomics data are unique compared to other high-dimensional datasets since they arise from imaging data and frequently exhibit strong correlations [165]. Therefore, reducing the number of features in radiomics analysis is crucial. Feature selection methods can be categorized into three groups, each having its specific advantages and disadvantages. Features selected by wrapper-based and embedded techniques may not generalize well to other classifiers because they rely on specific learning algorithms for feature selection. Filter-based techniques have lower computational complexity compared to embedded and wrapper-based techniques. The filter method directly selects features and has lower computational complexity than the embedded and wrapper methods, leading to a more stable feature set selection. However, as it does not interact with the learning algorithm, its accuracy may not be as high as the other two methods [166,167]. Various feature selection methods are available, and selecting the appropriate algorithm depends on various considerations. Researchers must have a comprehensive understanding of feature selection methods. However, the runtime feasibility of these methods can be a concern when dealing with high-dimensional datasets, as highlighted by Guyon et al. [168]. To achieve high performance while avoiding excessive complexity, researchers are advised to consider feature selection methods such as ANOVA, LASSO, and mRMR. If these three methods fail to produce the desired results, researchers should explore additional approaches.

Radiomics has shown its versatility across various medical conditions, with a particular focus on tumor diseases, but its application varies between tumor diseases and other medical conditions. In the context of tumor diseases, radiomics plays a crucial role in characterizing tumors, aiding in diagnosis, and assessing treatment response. For example, in lung cancer, radiomic features extracted from CT or PET images can determine tumor characteristics, differentiation, and even predict treatment outcomes and patient prognosis. In contrast, when applied to non-tumor conditions such as tuberculosis, radiomics assists in identifying pulmonary abnormalities and supporting diagnostics. Similarly, in pancreatitis, radiomics contributes to evaluating pancreatic morphology and density, aiding precise disease classification. Additionally, in stroke cases, radiomics reveals the extent and severity of brain lesions, providing valuable insights for tailored treatment strategies and predicting potential recovery paths. While radiomics holds significance in both contexts, its focus shifts from comprehensive characterization and prediction in tumor diseases to enhancing diagnostic accuracy and providing insights into disease manifestation in non-

tumor conditions. By addressing these differences, radiomics demonstrates its adaptability and potential to transform medical decision-making in diverse clinical scenarios.

The integration of imaging data with radiomics offers promise in advancing cancer research by enhancing screening, diagnosis, treatment decision-making, and follow-up [169]. However, despite the potential benefits of radiomics-based methods in cancer imaging, challenges related to their reproducibility and scalability persist. This paper aims to review the challenges associated with radiomics and provides an outlook to serve as a reference for future radiomics studies.

Radiomics faces various challenges, including data acquisition, repeatability, and reproducibility of radiomic features. Retrospective datasets are more accessible, making retrospective radiomics studies common [170]. However, utilizing retrospective data presents challenges regarding data accuracy for model training and validation. Pre-defined inclusion and exclusion criteria could introduce implicit biases in AI algorithms [171]. Furthermore, retrospective data are susceptible to non-harmonization issues due to the use of instruments from different providers, resulting in varying acquisition parameters, especially in multi-center studies. These differences in images may yield features influenced solely by technical discrepancies [172]. Sharing data and standardizing acquisition and reconstruction protocols can contribute to more reliable radiomics signatures, testable on external datasets, thereby addressing this concern [173]. To ensure result reproducibility, the IBSI was introduced to standardize the extraction of image biomarkers from acquired imaging. Nonetheless, conducting prospective studies is more demanding and time-consuming than retrospective studies, requiring long-term approval from pharmaceutical companies or cancer-collaborating organizations. Overall, combining data sharing with standardization of acquisition and reconstruction protocols may offer a potential solution to this issue and aid in identifying more robust radiomics features.

To achieve widespread acceptance, image biomarkers must address the challenge of interpretability, which poses an additional obstacle for radiomics. Radiomics models based on DL are often perceived as "black boxes" by clinicians, accurately predicting specific clinical outcomes but lacking interpretable explanations. To tackle this challenge, ongoing developments in radiomics techniques aim to merge the strengths of DL with the interpretability provided by hand-crafted methods. Interpretability is critical, particularly when evaluating image biomarkers for optimal therapy, as decisions guided by these biomarkers demand an interpretation rooted in pathophysiology [170]. Therefore, enhancing the interpretability of these models remains an ongoing area of research, with researchers exploring various tools [174].

The radiomics protocol, commonly used in cancer diagnosis, follows a signal-to-image-to-diagnosis approach. Accurately reconstructing visible images from the signal (raw data) obtained from medical devices is crucial for physicians to make accurate diagnoses. However, current image-based diagnostics often fail to fully utilize the abundant data in the signal, resulting in inadequate performance [175]. For instance, in CT imaging, the CT system collects raw data from the patient, which is then used to reconstruct images (signal-to-image). As a result, both AI-based and human-based diagnostic processes adopt a signal-to-image-to-knowledge approach. Medical images are prone to information distortion during both the acquisition and reconstruction processes [176]. Consequently, a novel approach to medical image analysis has emerged, emphasizing direct analysis of the raw data. Dong et al. [175] introduced an AI-based diagnostic scheme for pulmonary nodules that bypasses the reconstruction step and directly diagnoses from the signal. This groundbreaking research challenges conventional image-based diagnostics and may pave the way for a new era of AI-based diagnostics, offering a fresh direction for radiomics exploration.

5. Conclusions

Radiomics has showcased its diverse applications across various medical conditions, with a particular emphasis on tumor diseases. However, the application of radiomics significantly differs between tumor diseases and other medical conditions. In the context of tumor diseases, radiomics serves a pivotal role in characterizing tumors, aiding in diagnosis, and evaluating treatment response. For instance, in lung cancer, radiomics features extracted from CT or PET images facilitate the determination of tumor characteristics, differentiation, and even the prediction of treatment outcomes and patient prognosis. Conversely, the application of radiomics in non-tumor conditions diverges, primarily functioning as an assistive diagnostic tool. In diseases such as tuberculosis, radiomics aids in identifying pulmonary abnormalities and supporting diagnostic efforts. Similarly, in pancreatitis, radiomics contributes to assessing pancreatic morphology and density, aiding clinicians in precise disease classification. Moreover, in stroke cases, radiomics reveals the extent and severity of brain lesions, offering valuable insights for tailored treatment strategies and predicting potential recovery trajectories. While radiomics holds a profound influence in both contexts, its divergence lies in the specific clinical objectives. In tumor diseases, it serves as a comprehensive tool for characterization and prediction, whereas in non-tumor conditions, its emphasis shifts toward enhancing diagnostic accuracy and offering insights into disease manifestation. By bridging these differences, radiomics demonstrates its adaptability and potential to revolutionize medical decision-making in diverse clinical scenarios.

Radiomics, which encompasses intricate manual techniques and cutting-edge DL methods, represents a promising realm for the non-invasive identification of precise disease-related features. Its potential to support clinicians across tasks spanning from screening and diagnosis to treatment decision-making and post-treatment monitoring is indisputable. However, the truly groundbreaking facet of our study lies in the exhaustive exploration of the radiomics process. Commencing with the framework and categorization of feature selection methods, we unveil an array of techniques commonly employed in radiomics research. This panoramic perspective serves as a pivotal cornerstone for future advancements in the field. The central focus of this paper revolves around a pivotal aspect of radiomics: feature selection. This critical phase significantly enhances the performance and adaptability of radiomics models, thereby augmenting their clinical utility. Our study meticulously delves into diverse feature selection strategies, ranging from meticulous noise filtration to the strategic amalgamation of relevant features and even the introduction of features through embedding techniques. This comprehensive elucidation provides essential insights to guide researchers in making informed decisions amidst the intricate landscape of radiomics research. However, certain limitations within this study warrant consideration. First, despite our in-depth scrutiny of the radiomics process, there is room for further refinement and optimization of the application and effectiveness of feature selection methods. Second, while we discuss various feature selection strategies, the optimal selections across diverse disease types and clinical contexts require reinforcement through more empirical studies. Future endeavors should address these concerns to further amplify the applicability and advantages of radiomics within clinical practice. Notwithstanding the promising prospects of radiomics, researchers should remain attentive to potential obstacles lying ahead. Challenges pertaining to data quality, sample size, and the robustness of generalization capabilities demand attention. Furthermore, the urgency of developing standardized and validated radiomics studies cannot be underestimated. To surmount these challenges, a clear trajectory emerges: forthcoming studies must adhere to rigorous methodologies. This encompasses not only standardizing data acquisition and analysis procedures but also validating across diverse datasets. These collaborative efforts will assuredly fortify the position of radiomics within clinical practice and pave the way for enhanced patient care. In summation, situated at the crossroads of medical imaging and artificial intelligence, radiomics presents unprecedented opportunities within oncology research and clinical applications. As we overcome challenges, we are poised to

propel radiomics to the forefront, ushering in a new chapter in patient well-being and the advancement of medical science.

Author Contributions: Conceptualization, W.Z., Y.G. and Q.J.; Data curation, W.Z.; Formal analysis, W.Z. and Q.J.; Funding acquisition, Q.J.; Investigation, W.Z.; Methodology, W.Z., Y.G. and Q.J.; Project administration, W.Z. and Q.J.; Resources, W.Z.; Software, W.Z. and Y.G.; Supervision, Q.J.; Validation, Q.J.; Visualization, W.Z.; Writing—original draft, W.Z., Y.G. and Q.J.; Writing—review & editing, W.Z., Y.G. and Q.J. All authors have read and agreed to the published version of the manuscript.

Funding: This work was supported by the National Natural Science Foundation of China (No. 12061052), the Young Talents of Science and Technology in Universities of Inner Mongolia Autonomous Region (No. NJYT22090), the Natural Science Fund of Inner Mongolia Autonomous Region (No. 2020MS01002), the Innovative Research Team in Universities of Inner Mongolia Autonomous Region (No. NMGIRT2207), Inner Mongolia University Independent Research Project (2022-ZZ004), and the Network Information Center of Inner Mongolia University.

Data Availability Statement: No new data were created or analyzed in this study. Data sharing is not applicable to this article.

Acknowledgments: The authors would like to express their sincere appreciation to Caiying Wu, Guoqing Chen, and Xuemei Wang for their invaluable contributions to this research. Special gratitude is extended to Xuemei Wang for the generous support from the Inner Mongolia Autonomous Region Major Special Project Fund and Chen Guoqing's "111 Project" of Higher Education Talent Training in Inner Mongolia Autonomous Region program, which significantly contributed to the success of this work. Xuemei Wang's expert insights and guidance have greatly enhanced the credibility and professionalism of our research. Additionally, we would like to acknowledge the editors and technical staff at MDPI for their understanding and unwavering support throughout the preparation of this paper. Our sincere thanks are also extended to the reviewers for their insightful and pertinent comments, which have enriched the quality of our work.

Conflicts of Interest: The funders had no role in the design of the study; in the collection, analyses, or interpretation of data; in the writing of the manuscript; or in the decision to publish the results.

References

1. World Health Organization. Cancer—Key Facts. 2023. Available online: https://www.who.int/news-room/fact-sheets/detail/cancer (accessed on 8 March 2023).
2. Lambin, P.; Van Stiphout, R.G.; Starmans, M.H.; Rios-Velazquez, E.; Nalbantov, G.; Aerts, H.J.; Roelofs, E.; Van Elmpt, W.; Boutros, P.C.; Granone, P.; et al. Predicting outcomes in radiation oncology—Multifactorial decision support systems. *Nat. Rev. Clin. Oncol.* **2013**, *10*, 27–40. [CrossRef] [PubMed]
3. Chen, Q.; Zhang, L.; Liu, S.; You, J.; Chen, L.; Jin, Z.; Zhang, S.; Zhang, B. Radiomics in precision medicine for gastric cancer: Opportunities and challenges. *Eur. Radiol.* **2022**, *32*, 5852–5868. [CrossRef] [PubMed]
4. Lambin, P.; Rios-Velazquez, E.; Leijenaar, R.; Carvalho, S.; Van Stiphout, R.G.; Granton, P.; Zegers, C.M.; Gillies, R.; Boellard, R.; Dekker, A.; et al. Radiomics: Extracting more information from medical images using advanced feature analysis. *Eur. J. Cancer* **2012**, *48*, 441–446. [CrossRef]
5. Aerts, H.J.; Velazquez, E.R.; Leijenaar, R.T.; Parmar, C.; Grossmann, P.; Carvalho, S.; Bussink, J.; Monshouwer, R.; Haibe-Kains, B.; Rietveld, D.; et al. Decoding tumour phenotype by noninvasive imaging using a quantitative radiomics approach. *Nat. Commun.* **2014**, *5*, 4006. [CrossRef] [PubMed]
6. Hood, L.; Friend, S.H. Predictive, personalized, preventive, participatory (P4) cancer medicine. *Nat. Rev. Clin. Oncol.* **2011**, *8*, 184–187. [CrossRef]
7. Shen, C.; Liu, Z.; Guan, M.; Song, J.; Lian, Y.; Wang, S.; Tang, Z.; Dong, D.; Kong, L.; Wang, M.; et al. 2D and 3D CT radiomics features prognostic performance comparison in non-small cell lung cancer. *Transl. Oncol.* **2017**, *10*, 886–894. [CrossRef]
8. Peng, H.; Dong, D.; Fang, M.J.; Li, L.; Tang, L.L.; Chen, L.; Li, W.F.; Mao, Y.P.; Fan, W.; Liu, L.Z.; et al. Prognostic value of deep learning PET/CT-based radiomics: Potential role for future individual induction chemotherapy in advanced nasopharyngeal carcinoma. *Clin. Cancer Res.* **2019**, *25*, 4271–4279. [CrossRef]
9. Gillies, R.J.; Kinahan, P.E.; Hricak, H. Radiomics: Images are more than pictures, they are data. *Radiology* **2016**, *278*, 563–577. [CrossRef]
10. Chen, Q.; Xia, T.; Zhang, M.; Xia, N.; Liu, J.; Yang, Y. Radiomics in stroke neuroimaging: Techniques, applications, and challenges. *Aging Dis.* **2021**, *12*, 143. [CrossRef]
11. Liu, Z.; Wang, S.; Dong, D.; Wei, J.; Fang, C.; Zhou, X.; Sun, K.; Li, L.; Li, B.; Wang, M.; et al. The applications of radiomics in precision diagnosis and treatment of oncology: Opportunities and challenges. *Theranostics* **2019**, *9*, 1303. [CrossRef]

12. Wang, Y.; Zhang, L.; Qi, L.; Yi, X.; Li, M.; Zhou, M.; Chen, D.; Xiao, Q.; Wang, C.; Pang, Y.; et al. Machine learning: Applications and advanced progresses of radiomics in endocrine neoplasms. *J. Oncol.* **2021**, *2021*, 8615450. [CrossRef] [PubMed]
13. Gatenby, R.A.; Grove, O.; Gillies, R.J. Quantitative imaging in cancer evolution and ecology. *Radiology* **2013**, *269*, 8–14. [CrossRef] [PubMed]
14. Krizhevsky, A.; Sutskever, I.; Hinton, G.E. Imagenet classification with deep convolutional neural networks. *Commun. ACM* **2017**, *60*, 84–90. [CrossRef]
15. Soffer, S.; Ben-Cohen, A.; Shimon, O.; Amitai, M.M.; Greenspan, H.; Klang, E. Convolutional neural networks for radiologic images: A radiologist's guide. *Radiology* **2019**, *290*, 590–606. [CrossRef] [PubMed]
16. Zhao, X.; Liang, Y.J.; Zhang, X.; Wen, D.X.; Fan, W.; Tang, L.Q.; Dong, D.; Tian, J.; Mai, H.Q. Deep learning signatures reveal multiscale intratumor heterogeneity associated with biological functions and survival in recurrent nasopharyngeal carcinoma. *Eur. J. Nucl. Med. Mol. Imaging* **2022**, *49*, 2972–2982. [CrossRef]
17. Lambin, P.; Zindler, J.; Vanneste, B.G.; Van De Voorde, L.; Eekers, D.; Compter, I.; Panth, K.M.; Peerlings, J.; Larue, R.T.; Deist, T.M.; et al. Decision support systems for personalized and participative radiation oncology. *Adv. Drug Deliv. Rev.* **2017**, *109*, 131–153. [CrossRef]
18. Guiot, J.; Vaidyanathan, A.; Deprez, L.; Zerka, F.; Danthine, D.; Frix, A.N.; Lambin, P.; Bottari, F.; Tsoutzidis, N.; Miraglio, B.; et al. A review in radiomics: Making personalized medicine a reality via routine imaging. *Med. Res. Rev.* **2022**, *42*, 426–440. [CrossRef]
19. Yosinski, J.; Clune, J.; Bengio, Y.; Lipson, H. How transferable are features in deep neural networks? *Adv. Neural Inf. Process. Syst.* **2014**, *27*, 33203328.
20. Sheng, J.; Wumaier, A.; Li, Z. POISE: Efficient Cross-Domain Chinese Named Entity Recognization via Transfer Learning *Symmetry* **2020**, *12*, 1673. [CrossRef]
21. Christodoulidis, S.; Anthimopoulos, M.; Ebner, L.; Christe, A.; Mougiakakou, S. Multisource transfer learning with convolutional neural networks for lung pattern analysis. *IEEE J. Biomed. Health Inform.* **2016**, *21*, 76–84. [CrossRef]
22. Lambin, P.; Leijenaar, R.T.; Deist, T.M.; Peerlings, J.; De Jong, E.E.; Van Timmeren, J.; Sanduleanu, S.; Larue, R.T.; Even, A.J.; Jochems, A.; et al. Radiomics: The bridge between medical imaging and personalized medicine. *Nat. Rev. Clin. Oncol.* **2017**, *14*, 749–762. [CrossRef] [PubMed]
23. Dong, D.; Zhang, F.; Zhong, L.Z.; Fang, M.J.; Huang, C.L.; Yao, J.J.; Sun, Y.; Tian, J.; Ma, J.; Tang, L.L. Development and validation of a novel MR imaging predictor of response to induction chemotherapy in locoregionally advanced nasopharyngeal cancer: A randomized controlled trial substudy (NCT01245959). *BMC Med.* **2019**, *17*, 190. [CrossRef] [PubMed]
24. Wang, S.; Shi, J.; Ye, Z.; Dong, D.; Yu, D.; Zhou, M.; Liu, Y.; Gevaert, O.; Wang, K.; Zhu, Y.; et al. Predicting EGFR mutation status in lung adenocarcinoma on computed tomography image using deep learning. *Eur. Respir. J.* **2019**, *53*. [CrossRef]
25. Tian, P.; He, B.; Mu, W.; Liu, K.; Liu, L.; Zeng, H.; Liu, Y.; Jiang, L.; Zhou, P.; Huang, Z.; et al. Assessing PD-L1 expression in non-small cell lung cancer and predicting responses to immune checkpoint inhibitors using deep learning on computed tomography images. *Theranostics* **2021**, *11*, 2098. [CrossRef] [PubMed]
26. Zhang, S.; Song, G.; Zang, Y.; Jia, J.; Wang, C.; Li, C.; Tian, J.; Dong, D.; Zhang, Y. Non-invasive radiomics approach potentially predicts non-functioning pituitary adenomas subtypes before surgery. *Eur. Radiol.* **2018**, *28*, 3692–3701. [CrossRef]
27. Zhu, X.; Dong, D.; Chen, Z.; Fang, M.; Zhang, L.; Song, J.; Yu, D.; Zang, Y.; Liu, Z.; Shi, J.; et al. Radiomic signature as a diagnostic factor for histologic subtype classification of non-small cell lung cancer. *Eur. Radiol.* **2018**, *28*, 2772–2778. [CrossRef]
28. Gong, L.; Xu, M.; Fang, M.; Zou, J.; Yang, S.; Yu, X.; Xu, D.; Zhou, L.; Li, H.; He, B.; et al. Noninvasive prediction of high-grade prostate cancer via biparametric MRI radiomics. *J. Magn. Reson. Imaging* **2020**, *52*, 1102–1109. [CrossRef]
29. Li, J.; Dong, D.; Fang, M.; Wang, R.; Tian, J.; Li, H.; Gao, J. Dual-energy CT–based deep learning radiomics can improve lymph node metastasis risk prediction for gastric cancer. *Eur. Radiol.* **2020**, *30*, 2324–2333. [CrossRef]
30. Kan, Y.; Dong, D.; Zhang, Y.; Jiang, W.; Zhao, N.; Han, L.; Fang, M.; Zang, Y.; Hu, C.; Tian, J.; et al. Radiomic signature as a predictive factor for lymph node metastasis in early-stage cervical cancer. *J. Magn. Reson. Imaging* **2019**, *49*, 304–310. [CrossRef]
31. Liu, Y.; Fan, H.; Dong, D.; Liu, P.; He, B.; Meng, L.; Chen, J.; Chen, C.; Lang, J.; Tian, J. Computed tomography-based radiomic model at node level for the prediction of normal-sized lymph node metastasis in cervical cancer. *Transl. Oncol.* **2021**, *14*, 101113. [CrossRef]
32. Li, L.; Zhang, J.; Zhe, X.; Tang, M.; Zhang, X.; Lei, X.; Zhang, L. A meta-analysis of MRI-based radiomic features for predicting lymph node metastasis in patients with cervical cancer. *Eur. J. Radiol.* **2022**, *151*, 110243. [CrossRef]
33. Huang, Y.q.; Liang, C.h.; He, L.; Tian, J.; Liang, C.s.; Chen, X.; Ma, Z.l.; Liu, Z.y. Development and validation of a radiomics nomogram for preoperative prediction of lymph node metastasis in colorectal cancer. *J. Clin. Oncol.* **2016**, *34*, 2157–2164. [CrossRef]
34. Meng, Y.; Zhang, Y.; Dong, D.; Li, C.; Liang, X.; Zhang, C.; Wan, L.; Zhao, X.; Xu, K.; Zhou, C.; et al. Novel radiomic signature as a prognostic biomarker for locally advanced rectal cancer. *J. Magn. Reson. Imaging* **2018**, *48*, 605–614. [CrossRef] [PubMed]
35. Yang, L.; Dong, D.; Fang, M.; Zhu, Y.; Zang, Y.; Liu, Z.; Zhang, H.; Ying, J.; Zhao, X.; Tian, J. Can CT-based radiomics signature predict KRAS/NRAS/BRAF mutations in colorectal cancer? *Eur. Radiol.* **2018**, *28*, 2058–2067. [CrossRef]
36. Liang, C.; Huang, Y.; He, L.; Chen, X.; Ma, Z.; Dong, D.; Tian, J.; Liang, C.; Liu, Z. The development and validation of a CT-based radiomics signature for the preoperative discrimination of stage I-II and stage III-IV colorectal cancer. *Oncotarget* **2016**, *7*, 31401. [CrossRef] [PubMed]

37. Bedrikovetski, S.; Dudi-Venkata, N.N.; Kroon, H.M.; Seow, W.; Vather, R.; Carneiro, G.; Moore, J.W.; Sammour, T. Artificial intelligence for pre-operative lymph node staging in colorectal cancer: A systematic review and meta-analysis. *BMC Cancer* **2021**, *21*, 1058. [CrossRef]
38. Jia, L.L.; Zhao, J.X.; Zhao, L.P.; Tian, J.H.; Huang, G. Current status and quality of radiomic studies for predicting KRAS mutations in colorectal cancer patients: A systematic review and meta-analysis. *Eur. J. Radiol.* **2023**, *158*, 110640. [CrossRef]
39. Dong, D.; Fang, M.J.; Tang, L.; Shan, X.H.; Gao, J.B.; Giganti, F.; Wang, R.P.; Chen, X.; Wang, X.X.; Palumbo, D.; et al. Deep learning radiomic nomogram can predict the number of lymph node metastasis in locally advanced gastric cancer: An international multicenter study. *Ann. Oncol.* **2020**, *31*, 912–920. [CrossRef] [PubMed]
40. Zhang, L.; Dong, D.; Zhong, L.; Li, C.; Hu, C.; Yang, X.; Liu, Z.; Wang, R.; Zhou, J.; Tian, J. Multi-focus network to decode imaging phenotype for overall survival prediction of Gastric cancer patients. *IEEE J. Biomed. Health Inform.* **2021**, *25*, 3933–3942. [CrossRef]
41. Li, C.; Qin, Y.; Zhang, W.H.; Jiang, H.; Song, B.; Bashir, M.R.; Xu, H.; Duan, T.; Fang, M.; Zhong, L.; et al. Deep learning-based AI model for signet-ring cell carcinoma diagnosis and chemotherapy response prediction in gastric cancer. *Med. Phys.* **2022**, *49*, 1535–1546. [CrossRef]
42. Wang, S.; Feng, C.; Dong, D.; Li, H.; Zhou, J.; Ye, Y.; Liu, Z.; Tian, J.; Wang, Y. Preoperative computed tomography-guided disease-free survival prediction in gastric cancer: A multicenter radiomics study. *Med. Phys.* **2020**, *47*, 4862–4871. [CrossRef] [PubMed]
43. Dong, D.; Tang, L.; Li, Z.Y.; Fang, M.J.; Gao, J.B.; Shan, X.H.; Ying, X.J.; Sun, Y.S.; Fu, J.; Wang, X.X.; et al. Development and validation of an individualized nomogram to identify occult peritoneal metastasis in patients with advanced gastric cancer. *Ann. Oncol.* **2019**, *30*, 431–438. [CrossRef] [PubMed]
44. Zhang, F.; Wu, G.; Chen, N.; Li, R. The predictive value of radiomics-based machine learning for peritoneal metastasis in gastric cancer patients: A systematic review and meta-analysis. *Front. Oncol.* **2023**, *13*, 1196053. [CrossRef] [PubMed]
45. Li, Z.; Li, H.; Wang, S.; Dong, D.; Yin, F.; Chen, A.; Wang, S.; Zhao, G.; Fang, M.; Tian, J.; et al. MR-based radiomics nomogram of cervical cancer in prediction of the lymph-vascular space invasion preoperatively. *J. Magn. Reson. Imaging* **2019**, *49*, 1420–1426. [CrossRef]
46. Fang, M.; Kan, Y.; Dong, D.; Yu, T.; Zhao, N.; Jiang, W.; Zhong, L.; Hu, C.; Luo, Y.; Tian, J. Multi-habitat based radiomics for the prediction of treatment response to concurrent chemotherapy and radiation therapy in locally advanced cervical cancer. *Front. Oncol.* **2020**, *10*, 563. [CrossRef] [PubMed]
47. Chen, J.; He, B.; Dong, D.; Liu, P.; Duan, H.; Li, W.; Li, P.; Wang, L.; Fan, H.; Wang, S.; et al. Noninvasive CT radiomic model for preoperative prediction of lymph node metastasis in early cervical carcinoma. *Br. J. Radiol.* **2020**, *93*, 20190558. [CrossRef]
48. Ren, J.; Li, Y.; Liu, X.Y.; Zhao, J.; He, Y.L.; Jin, Z.Y.; Xue, H.D. Diagnostic performance of ADC values and MRI-based radiomics analysis for detecting lymph node metastasis in patients with cervical cancer: A systematic review and meta-analysis. *Eur. J. Radiol.* **2022**, *156*, 110504. [CrossRef]
49. Xie, T.; Wang, X.; Li, M.; Tong, T.; Yu, X.; Zhou, Z. Pancreatic ductal adenocarcinoma: A radiomics nomogram outperforms clinical model and TNM staging for survival estimation after curative resection. *Eur. Radiol.* **2020**, *30*, 2513–2524. [CrossRef]
50. Gao, Y.; Cheng, S.; Zhu, L.; Wang, Q.; Deng, W.; Sun, Z.; Wang, S.; Xue, H. A systematic review of prognosis predictive role of radiomics in pancreatic cancer: Heterogeneity markers or statistical tricks? *Eur. Radiol.* **2022**, *32*, 8443–8452. [CrossRef]
51. Zhong, J.; Hu, Y.; Xing, Y.; Ge, X.; Ding, D.; Zhang, H.; Yao, W. A systematic review of radiomics in pancreatitis: Applying the evidence level rating tool for promoting clinical transferability. *Insights Imaging* **2022**, *13*, 139. [CrossRef]
52. Zhong, L.; Dong, D.; Fang, X.; Zhang, F.; Zhang, N.; Zhang, L.; Fang, M.; Jiang, W.; Liang, S.; Li, C.; et al. A deep learning-based radiomic nomogram for prognosis and treatment decision in advanced nasopharyngeal carcinoma: A multicentre study. *EBioMedicine* **2021**, *70*, 103522. [CrossRef] [PubMed]
53. Zhang, L.; Zhou, H.; Gu, D.; Tian, J.; Zhang, B.; Dong, D.; Mo, X.; Liu, J.; Luo, X.; Pei, S.; et al. Radiomic nomogram: Pretreatment evaluation of local recurrence in nasopharyngeal carcinoma based on MR imaging. *J. Cancer* **2019**, *10*, 4217. [CrossRef] [PubMed]
54. Zhang, B.; Tian, J.; Dong, D.; Gu, D.; Dong, Y.; Zhang, L.; Lian, Z.; Liu, J.; Luo, X.; Pei, S.; et al. Radiomics Features of Multiparametric MRI as Novel Prognostic Factors in Advanced Nasopharyngeal CarcinomaPretreatment Radiomics for Nasopharyngeal Carcinoma. *Clin. Cancer Res.* **2017**, *23*, 4259–4269. [CrossRef] [PubMed]
55. Zhong, L.Z.; Fang, X.L.; Dong, D.; Peng, H.; Fang, M.J.; Huang, C.L.; He, B.X.; Lin, L.; Ma, J.; Tang, L.L.; et al. A deep learning MR-based radiomic nomogram may predict survival for nasopharyngeal carcinoma patients with stage T3N1M0. *Radiother. Oncol.* **2020**, *151*, 1–9. [CrossRef]
56. Lee, S.; Choi, Y.; Seo, M.K.; Jang, J.; Shin, N.Y.; Ahn, K.J.; Kim, B.S. Magnetic Resonance Imaging-Based Radiomics for the Prediction of Progression-Free Survival in Patients with Nasopharyngeal Carcinoma: A Systematic Review and Meta-Analysis. *Cancers* **2022**, *14*, 653. [CrossRef]
57. Yang, C.; Jiang, Z.; Cheng, T.; Zhou, R.; Wang, G.; Jing, D.; Bo, L.; Huang, P.; Wang, J.; Zhang, D.; et al. Radiomics for Predicting Response of Neoadjuvant Chemotherapy in Nasopharyngeal Carcinoma: A Systematic Review and Meta-Analysis. *Front. Oncol.* **2022**, *12*, 893103. [CrossRef]
58. Park, H.; Lim, Y.; Ko, E.S.; Cho, H.h.; Lee, J.E.; Han, B.K.; Ko, E.Y.; Choi, J.S.; Park, K.W. Radiomics Signature on Magnetic Resonance Imaging: Association with Disease-Free Survival in Patients with Invasive Breast CancerRadiomics Signature on MRI for DFS in Invasive Breast Cancer. *Clin. Cancer Res.* **2018**, *24*, 4705–4714. [CrossRef]

59. Han, L.; Zhu, Y.; Liu, Z.; Yu, T.; He, C.; Jiang, W.; Kan, Y.; Dong, D.; Tian, J.; Luo, Y. Radiomic nomogram for prediction of axillary lymph node metastasis in breast cancer. *Eur. Radiol.* **2019**, *29*, 3820–3829. [CrossRef]
60. Jiang, M.; Li, C.L.; Luo, X.M.; Chuan, Z.R.; Lv, W.Z.; Li, X.; Cui, X.W.; Dietrich, C.F. Ultrasound-based deep learning radiomics in the assessment of pathological complete response to neoadjuvant chemotherapy in locally advanced breast cancer. *Eur. J. Cancer* **2021**, *147*, 95–105. [CrossRef]
61. Pesapane, F.; Agazzi, G.M.; Rotili, A.; Ferrari, F.; Cardillo, A.; Penco, S.; Dominelli, V.; D'Ecclesiis, O.; Vignati, S.; Raimondi, S.; et al. Prediction of the Pathological Response to Neoadjuvant Chemotherapy in Breast Cancer Patients with MRI-Radiomics: A Systematic Review and Meta-analysis. *Curr. Probl. Cancer* **2022**, *46*, 100883. [CrossRef]
62. Liang, X.; Yu, X.; Gao, T. Machine learning with magnetic resonance imaging for prediction of response to neoadjuvant chemotherapy in breast cancer: A systematic review and meta-analysis. *Eur. J. Radiol.* **2022**, *150*, 110247. [CrossRef] [PubMed]
63. Zhou, H.; Dong, D.; Chen, B.; Fang, M.; Cheng, Y.; Gan, Y.; Zhang, R.; Zhang, L.; Zang, Y.; Liu, Z.; et al. Diagnosis of distant metastasis of lung cancer: Based on clinical and radiomic features. *Transl. Oncol.* **2018**, *11*, 31–36. [CrossRef] [PubMed]
64. Chen, J.; Zeng, H.; Zhang, C.; Shi, Z.; Dekker, A.; Wee, L.; Bermejo, I. Lung cancer diagnosis using deep attention-based multiple instance learning and radiomics. *Med. Phys.* **2022**, *49*, 3134–3143. [CrossRef] [PubMed]
65. He, B.; Dong, D.; She, Y.; Zhou, C.; Fang, M.; Zhu, Y.; Zhang, H.; Huang, Z.; Jiang, T.; Tian, J.; et al. Predicting response to immunotherapy in advanced non-small-cell lung cancer using tumor mutational burden radiomic biomarker. *J. Immunother. Cancer* **2020**, *8*, e000550. [CrossRef]
66. Zhang, L.; Chen, B.; Liu, X.; Song, J.; Fang, M.; Hu, C.; Dong, D.; Li, W.; Tian, J. Quantitative biomarkers for prediction of epidermal growth factor receptor mutation in non-small cell lung cancer. *Transl. Oncol.* **2018**, *11*, 94–101. [CrossRef] [PubMed]
67. Zheng, X.; He, B.; Hu, Y.; Ren, M.; Chen, Z.; Zhang, Z.; Ma, J.; Ouyang, L.; Chu, H.; Gao, H.; et al. Diagnostic Accuracy of Deep Learning and Radiomics in Lung Cancer Staging: A Systematic Review and Meta-Analysis. *Front. Public Health* **2022**, *10*, 938113. [CrossRef]
68. Gabelloni, M.; Faggioni, L.; Fusco, R.; Simonetti, I.; De Muzio, F.; Giacobbe, G.; Borgheresi, A.; Bruno, F.; Cozzi, D.; Grassi, F.; et al. Radiomics in Lung Metastases: A Systematic Review. *J. Pers. Med.* **2023**, *13*, 225. [CrossRef]
69. Gu, H.; Zhang, X.; Di Russo, P.; Zhao, X.; Xu, T. The current state of radiomics for meningiomas: Promises and challenges. *Front. Oncol.* **2020**, *10*, 567736. [CrossRef]
70. Reiazi, R.; Abbas, E.; Famiyeh, P.; Rezaie, A.; Kwan, J.Y.; Patel, T.; Bratman, S.V.; Tadic, T.; Liu, F.F.; Haibe-Kains, B. The impact of the variation of imaging parameters on the robustness of computed tomography radiomic features: A review. *Comput. Biol. Med.* **2021**, *133*, 104400. [CrossRef]
71. Cui, Y.; Zhang, J.; Li, Z.; Wei, K.; Lei, Y.; Ren, J.; Wu, L.; Shi, Z.; Meng, X.; Yang, X.; et al. A CT-based deep learning radiomics nomogram for predicting the response to neoadjuvant chemotherapy in patients with locally advanced gastric cancer: A multicenter cohort study. *EClinicalMedicine* **2022**, *46*, 101348. [CrossRef]
72. Zhang, L.; Dong, D.; Zhang, W.; Hao, X.; Fang, M.; Wang, S.; Li, W.; Liu, Z.; Wang, R.; Zhou, J.; et al. A deep learning risk prediction model for overall survival in patients with gastric cancer: A multicenter study. *Radiother. Oncol.* **2020**, *150*, 73–80. [CrossRef] [PubMed]
73. Wu, X.; Dong, D.; Zhang, L.; Fang, M.; Zhu, Y.; He, B.; Ye, Z.; Zhang, M.; Zhang, S.; Tian, J. Exploring the predictive value of additional peritumoral regions based on deep learning and radiomics: A multicenter study. *Med. Phys.* **2021**, *48*, 2374–2385. [CrossRef] [PubMed]
74. Sullivan, D.C.; Obuchowski, N.A.; Kessler, L.G.; Raunig, D.L.; Gatsonis, C.; Huang, E.P.; Kondratovich, M.; McShane, L.M.; Reeves, A.P.; Barboriak, D.P.; et al. Metrology standards for quantitative imaging biomarkers. *Radiology* **2015**, *277*, 813–825. [CrossRef]
75. deSouza, N.M.; Achten, E.; Alberich-Bayarri, A.; Bamberg, F.; Boellaard, R.; Clément, O.; Fournier, L.; Gallagher, F.; Golay, X.; Heussel, C.P.; et al. Validated imaging biomarkers as decision-making tools in clinical trials and routine practice: Current status and recommendations from the EIBALL* subcommittee of the European Society of Radiology (ESR). *Insights Imaging* **2019**, *10*, 87. [CrossRef] [PubMed]
76. Avery, E.; Sanelli, P.C.; Aboian, M.; Payabvash, S. Radiomics: A Primer on Processing Workflow and Analysis. *Semin. Ultrasound CT MRI* **2022**, *43*, 142–146. [CrossRef] [PubMed]
77. Bartko, J.J. The intraclass correlation coefficient as a measure of reliability. *Psychol. Rep.* **1966**, *19*, 3–11. [CrossRef] [PubMed]
78. Fedorov, A.; Beichel, R.; Kalpathy-Cramer, J.; Finet, J.; Fillion-Robin, J.C.; Pujol, S.; Bauer, C.; Jennings, D.; Fennessy, F.; Sonka, M.; et al. 3D Slicer as an image computing platform for the Quantitative Imaging Network. *Magn. Reson. Imaging* **2012**, *30*, 1323–1341. [CrossRef]
79. Yushkevich, P.A.; Gao, Y.; Gerig, G. ITK-SNAP: An interactive tool for semi-automatic segmentation of multi-modality biomedical images. In Proceedings of the 2016 38th Annual International Conference of the IEEE Engineering in Medicine and Biology Society (EMBC), Orlando, FL, USA, 16–20 August 2016; IEEE: Piscataway, NJ, USA, **2016**; pp. 3342–3345.
80. Girish, V.; Vijayalakshmi, A. Affordable image analysis using NIH Image/ImageJ. *Indian J. Cancer* **2004**, *41*, 47.
81. Tian, J.; Xue, J.; Dai, Y.; Chen, J.; Zheng, J. A novel software platform for medical image processing and analyzing. *IEEE Trans. Inf. Technol. Biomed.* **2008**, *12*, 800–812. [CrossRef]
82. Dong, D.; Tian, J.; Dai, Y.; Yan, G.; Yang, F.; Wu, P. Unified reconstruction framework for multi-modal medical imaging. *J. X-ray Sci. Technol.* **2011**, *19*, 111–126. [CrossRef]

83. Wang, S.; Zhou, M.; Liu, Z.; Liu, Z.; Gu, D.; Zang, Y.; Dong, D.; Gevaert, O.; Tian, J. Central focused convolutional neural networks: Developing a data-driven model for lung nodule segmentation. *Med. Image Anal.* **2017**, *40*, 172–183. [CrossRef]
84. Yang, S.; Kweon, J.; Roh, J.H.; Lee, J.H.; Kang, H.; Park, L.J.; Kim, D.J.; Yang, H.; Hur, J.; Kang, D.Y.; et al. Deep learning segmentation of major vessels in X-ray coronary angiography. *Sci. Rep.* **2019**, *9*, 16897. [CrossRef] [PubMed]
85. Yu, S.; Wang, Q.; Ru, C.; Pang, M. Location detection of key areas in medical images based on Haar-like fusion contour feature learning. *Technol. Health Care* **2020**, *28*, 391–399. [CrossRef] [PubMed]
86. Chen, X.; Pan, L. A survey of graph cuts/graph search based medical image segmentation. *IEEE Rev. Biomed. Eng.* **2018**, *11*, 112–124. [CrossRef] [PubMed]
87. Zanaty, E.; Afifi, A. A watershed approach for improving medical image segmentation. *Comput. Methods Biomech. Biomed. Eng.* **2013**, *16*, 1262–1272. [CrossRef] [PubMed]
88. Hesamian, M.H.; Jia, W.; He, X.; Kennedy, P. Deep Learning Techniques for Medical Image Segmentation: Achievements and Challenges. *J. Digit. Imaging* **2019**, *32*, 582–596. [CrossRef]
89. Ronneberger, O.; Fischer, P.; Brox, T. U-net: Convolutional networks for biomedical image segmentation. In Proceedings of the Medical Image Computing and Computer-Assisted Intervention–MICCAI 2015: 18th International Conference, Munich, Germany, 5–9 October 2015; Proceedings, Part III 18; Springer: Cham, Switzerland, 2015; pp. 234–241.
90. Zhang, J.; Qin, Q.; Ye, Q.; Ruan, T. ST-Unet: Swin Transformer boosted U-Net with Cross-Layer Feature Enhancement for medical image segmentation. *Comput. Biol. Med.* **2023**, *153*, 106516. [CrossRef] [PubMed]
91. Zhou, Z.; Rahman Siddiquee, M.M.; Tajbakhsh, N.; Liang, J. Unet++: A nested u-net architecture for medical image segmentation. In Proceedings of the Deep Learning in Medical Image Analysis and Multimodal Learning for Clinical Decision Support: 4th International Workshop, DLMIA 2018, and 8th International Workshop, ML-CDS 2018, Held in Conjunction with MICCAI 2018, Granada, Spain, 20 September 2018; Proceedings 4; Springer: Cham, Switzerland, 2018; pp. 3–11.
92. Li, J.; Liu, K.; Hu, Y.; Zhang, H.; Heidari, A.A.; Chen, H.; Zhang, W.; Algarni, A.D.; Elmannai, H. Eres-UNet++: Liver CT image segmentation based on high-efficiency channel attention and Res-UNet++. *Comput. Biol. Med.* **2023**, *158*, 106501. [CrossRef] [PubMed]
93. Gu, Z.; Cheng, J.; Fu, H.; Zhou, K.; Hao, H.; Zhao, Y.; Zhang, T.; Gao, S.; Liu, J. Ce-net: Context encoder network for 2d medical image segmentation. *IEEE Trans. Med. Imaging* **2019**, *38*, 2281–2292. [CrossRef] [PubMed]
94. Fang, X.; Yan, P. Multi-organ segmentation over partially labeled datasets with multi-scale feature abstraction. *IEEE Trans. Med. Imaging* **2020**, *39*, 3619–3629. [CrossRef]
95. Van Griethuysen, J.J.; Fedorov, A.; Parmar, C.; Hosny, A.; Aucoin, N.; Narayan, V.; Beets-Tan, R.G.; Fillion-Robin, J.C.; Pieper, S.; Aerts, H.J. Computational radiomics system to decode the radiographic phenotype. *Cancer Res.* **2017**, *77*, e104–e107. [CrossRef] [PubMed]
96. Zwanenburg, A.; Vallières, M.; Abdalah, M.A.; Aerts, H.J.; Andrearczyk, V.; Apte, A.; Ashrafinia, S.; Bakas, S.; Beukinga, R.J.; Boellaard, R.; et al. The image biomarker standardization initiative: Standardized quantitative radiomics for high-throughput image-based phenotyping. *Radiology* **2020**, *295*, 328–338. [CrossRef]
97. Rizzo, S.; Botta, F.; Raimondi, S.; Origgi, D.; Fanciullo, C.; Morganti, A.G.; Bellomi, M. Radiomics: The facts and the challenges of image analysis. *Eur. Radiol. Exp.* **2018**, *2*, 36. [CrossRef] [PubMed]
98. Ergen, B.; Baykara, M. Texture based feature extraction methods for content based medical image retrieval systems. *Bio-Med. Mater. Eng.* **2014**, *24*, 3055–3062. [CrossRef]
99. Haralick, R.M.; Shanmugam, K.; Dinstein, I.H. Textural features for image classification. *IEEE Trans. Syst. Man Cybern.* **1973**, *SMC-3*, 610–621. [CrossRef]
100. Oliver, J.A.; Budzevich, M.; Zhang, G.G.; Dilling, T.J.; Latifi, K.; Moros, E.G. Variability of Image Features Computed from Conventional and Respiratory-Gated PET/CT Images of Lung Cancer. *Transl. Oncol.* **2015**, *8*, 524–534. [CrossRef]
101. Chu, A.; Sehgal, C.M.; Greenleaf, J.F. Use of gray value distribution of run lengths for texture analysis. *Pattern Recognit. Lett.* **1990**, *11*, 415–419. [CrossRef]
102. Galloway, M.M. Texture analysis using gray level run lengths. *Comput. Graph. Image Process.* **1975**, *4*, 172–179. [CrossRef]
103. Thibault, G.; Fertil, B.; Navarro, C.; Pereira, S.; Cau, P.; Levy, N.; Sequeira, J.; Mari, J.-L. Shape and Texture Indexes Application to Cell Nuclei Classification. *Int. J. Pattern Recognit. Artif. Intell.* **2013**, *27*, 1357002. [CrossRef]
104. Amadasun, M.; King, R. Textural features corresponding to textural properties. *IEEE Trans. Syst. Man Cybern.* **1989**, *19*, 1264–1274. [CrossRef]
105. Haralick, R.M. Statistical and structural approaches to texture. *Proc. IEEE* **1979**, *67*, 786–804. [CrossRef]
106. Bera, K.; Braman, N.; Gupta, A.; Velcheti, V.; Madabhushi, A. Predicting cancer outcomes with radiomics and artificial intelligence in radiology. *Nat. Rev. Clin. Oncol.* **2022**, *19*, 132–146. [CrossRef] [PubMed]
107. Jiang, Y.; Liang, X.; Wang, W.; Chen, C.; Yuan, Q.; Zhang, X.; Li, N.; Chen, H.; Yu, J.; Xie, Y.; et al. Noninvasive prediction of occult peritoneal metastasis in gastric cancer using deep learning. *JAMA Netw. Open* **2021**, *4*, e2032269. [CrossRef]
108. Li, Z.; Zhang, J.; Tan, T.; Teng, X.; Sun, X.; Zhao, H.; Liu, L.; Xiao, Y.; Lee, B.; Li, Y.; et al. Deep learning methods for lung cancer segmentation in whole-slide histopathology images—The acdc@ lunghp challenge 2019. *IEEE J. Biomed. Health Inform.* **2020**, *25*, 429–440. [CrossRef]
109. Liang, B.; Li, H.; Su, M.; Li, X.; Shi, W.; Wang, X. Detecting adversarial image examples in deep neural networks with adaptive noise reduction. *IEEE Trans. Dependable Secur. Comput.* **2018**, *18*, 72–85. [CrossRef]

110. Chen, T.; Guestrin, C. Xgboost: A scalable tree boosting system. In Proceedings of the 22nd acm sigkdd International Conference on Knowledge Discovery and Data Mining, San Francisco, CA, USA, 13–17 August 2016; pp. 785–794.
111. Belgiu, M.; Drăguţ, L. Random forest in remote sensing: A review of applications and future directions. *ISPRS J. Photogramm. Remote Sens.* **2016**, *114*, 24–31. [CrossRef]
112. Breiman, L. Random forests. *Mach. Learn.* **2001**, *45*, 5–32. [CrossRef]
113. Murphy, K.P. Naive bayes classifiers. *Univ. Br. Columbia* **2006**, *18*, 1–8.
114. Suthaharan, S.; Suthaharan, S. Support vector machine. In *Machine Learning Models and Algorithms for Big Data Classification: Thinking with Examples for Effective Learning*; Springer: New York, NY, USA, 2016; pp. 207–235.
115. Shiri, I.; Salimi, Y.; Pakbin, M.; Hajianfar, G.; Avval, A.H.; Sanaat, A.; Mostafaei, S.; Akhavanallaf, A.; Saberi, A.; Mansouri, Z.; et al. COVID-19 prognostic modeling using CT radiomic features and machine learning algorithms: Analysis of a multi-institutional dataset of 14,339 patients. *Comput. Biol. Med.* **2022**, *145*, 105467. [CrossRef]
116. Park, J.E.; Kim, D.; Kim, H.S.; Park, S.Y.; Kim, J.Y.; Cho, S.J.; Shin, J.H.; Kim, J.H. Quality of science and reporting of radiomics in oncologic studies: Room for improvement according to radiomics quality score and TRIPOD statement. *Eur. Radiol.* **2020**, *30*, 523–536. [CrossRef]
117. Baeßler, B.; Weiss, K.; Dos Santos, D.P. Robustness and reproducibility of radiomics in magnetic resonance imaging: A phantom study. *Investig. Radiol.* **2019**, *54*, 221–228. [CrossRef] [PubMed]
118. Bernatz, S.; Zhdanovich, Y.; Ackermann, J.; Koch, I.; Wild, P.J.; Dos Santos, D.P.; Vogl, T.J.; Kaltenbach, B.; Rosbach, N. Impact of rescanning and repositioning on radiomic features employing a multi-object phantom in magnetic resonance imaging. *Sci. Rep.* **2021**, *11*, 14248. [CrossRef]
119. Pinto dos Santos, D.; Dietzel, M.; Baessler, B. A decade of radiomics research: Are images really data or just patterns in the noise? *Eur. Radiol.* **2021**, *31*, 1–4. [CrossRef]
120. Demircioğlu, A. Benchmarking feature selection methods in radiomics. *Investig. Radiol.* **2022**, *57*, 433–443. [CrossRef] [PubMed]
121. Dash, M.; Liu, H. Feature selection for classification. *Intell. Data Anal.* **1997**, *1*, 131–156. [CrossRef]
122. Yu, L.; Liu, H. Efficient feature selection via analysis of relevance and redundancy. *J. Mach. Learn. Res.* **2004**, *5*, 1205–1224.
123. Li, Y.; Li, T.; Liu, H. Recent advances in feature selection and its applications. *Knowl. Inf. Syst.* **2017**, *53*, 551–577. [CrossRef]
124. Peng, H.; Long, F.; Ding, C. Feature selection based on mutual information criteria of max-dependency, max-relevance, and min-redundancy. *IEEE Trans. Pattern Anal. Mach. Intell.* **2005**, *27*, 1226–1238. [CrossRef]
125. Hall, M.A. Correlation-based Feature Selection for Discrete and Numeric Class Machine Learning. In Proceedings of the International Conference on Machine Learning, Stanford, CA, USA, 29 June–2 July 1999; pp. 1–8.
126. Yu, L.; Liu, H. Feature selection for high-dimensional data: A fast correlation-based filter solution. In Proceedings of the 20th International Conference on Machine Learning (ICML-03), Washington, DC, USA, 21–24 August 2003; pp. 856–863.
127. Anukrishna, P.; Paul, V. A review on feature selection for high dimensional data. In Proceedings of the 2017 International Conference on Inventive Systems and Control (ICISC), Coimbatore, India, 19–20 January 2017; IEEE: Piscataway, NJ, USA, 2017; pp. 1–4.
128. Alduailij, M.; Khan, Q.W.; Tahir, M.; Sardaraz, M.; Alduailij, M.; Malik, F. Machine-Learning-Based DDoS Attack Detection Using Mutual Information and Random Forest Feature Importance Method. *Symmetry* **2022**, *14*, 1095. [CrossRef]
129. Cohen, I.; Huang, Y.; Chen, J.; Benesty, J.; Benesty, J.; Chen, J.; Huang, Y.; Cohen, I. Pearson correlation coefficient. *Noise Reduct. Speech Process.* **2009**, *2*, 1–4.
130. Yu, H.; Meng, X.; Chen, H.; Han, X.; Fan, J.; Gao, W.; Du, L.; Chen, Y.; Wang, Y.; Liu, X.; et al. Correlation between mammographic radiomics features and the level of tumor-infiltrating lymphocytes in patients with triple-negative breast cancer. *Front. Oncol.* **2020**, *10*, 412. [CrossRef] [PubMed]
131. Spearman, C. The proof and measurement of association between two things. *Amer. J. Psychol.* **1904**, *15*, 72–101. [CrossRef]
132. Chelvan, P.M.; Perumal, K. A comparative analysis of feature selection stability measures. In Proceedings of the 2017 International Conference on Trends in Electronics and Informatics (ICEI), Tirunelveli, India, 11–12 May 2017; IEEE: Piscataway, NJ, USA, 2017; pp. 124–128.
133. Larson, M.G. Analysis of variance. *Circulation* **2008**, *117*, 115–121. [CrossRef] [PubMed]
134. Wang, Z.; Yang, G.; Wang, X.; Cao, Y.; Jiao, W.; Niu, H. A combined model based on CT radiomics and clinical variables to predict uric acid calculi which have a good accuracy. *Urolithiasis* **2023**, *51*, 37. [CrossRef] [PubMed]
135. Liu, H.; Setiono, R. Chi2: Feature selection and discretization of numeric attributes. In Proceedings of the 7th IEEE International Conference on Tools with Artificial Intelligence, Herndon, VA, USA, 5–8 November 1995; IEEE: Piscataway, NJ, USA, 1995; pp. 388–391.
136. Plackett, R.L. Karl Pearson and the chi-squared test. *Int. Stat. Rev. Int. De Statistique* **1983**, *51*, 59–72. [CrossRef]
137. Vergara, J.R.; Estévez, P.A. A review of feature selection methods based on mutual information. *Neural Comput. Appl.* **2014**, *24*, 175–186. [CrossRef]
138. Wu, Y.; Liu, B.; Wu, W.; Lin, Y.; Yang, C.; Wang, M. Grading glioma by radiomics with feature selection based on mutual information. *J. Ambient. Intell. Humaniz. Comput.* **2018**, *9*, 1671–1682. [CrossRef]
139. Gan, M.; Zhang, L. Iteratively local fisher score for feature selection. *Appl. Intell.* **2021**, *51*, 6167–6181. [CrossRef]

140. Zeng, X.; Chen, Y.W.; Tao, C. Feature selection using recursive feature elimination for handwritten digit recognition. In Proceedings of the 2009 Fifth International Conference on Intelligent Information Hiding and Multimedia Signal Processing, Kyoto, Japan, 12–14 September 2009; IEEE: Piscataway, NJ, USA, 2009; pp. 1205–1208.
141. Bundy, A.; Wallen, L. Breadth-first search. In *Catalogue of Artificial Intelligence Tools*; Springer: Berlin/Heidelberg, Germany, 1984; pp.13–13.
142. Dechter, R.; Pearl, J. Generalized best-first search strategies and the optimality of A. *J. ACM (JACM)* **1985**, *32*, 505–536. [CrossRef]
143. Morris, R. Tapered floating point: A new floating-point representation. *IEEE Trans. Comput.* **1971**, *100*, 1578–1579. [CrossRef]
144. Theodoridis, S.; Pikrakis, A.; Koutroumbas, K.; Cavouras, D. *Introduction to Pattern Recognition: A Matlab Approach*; Academic Press: Cambridge, MA, USA, **2010**.
145. Mustafa, S. Feature selection using sequential backward method in melanoma recognition. In Proceedings of the 2017 13th International Conference on Electronics, Computer and Computation (ICECCO), Abuja, Nigeria, 28–29 November 2017; IEEE: Piscataway, NJ, USA, 2017; pp. 1–4.
146. Doak, J. *An Evaluation of Feature Selection Methods and Their Application to Computer Security*; Technical Report CSE-92-18; University of California, Department of Computer Science: Berkeley, CA, USA, 1992.
147. Webb, A.R. *Statistical Pattern Recognition*; John Wiley & Sons: Hoboken, NJ, USA, 2003.
148. Pudil, P.; Novovičová, J.; Kittler, J. Floating search methods in feature selection. *Pattern Recognit. Lett.* **1994**, *15*, 1119–1125. [CrossRef]
149. Grabczewski, K.; Jankowski, N. Feature selection with decision tree criterion. In Proceedings of the Fifth International Conference on Hybrid Intelligent Systems (HIS'05), Rio de Janeiro, Brazil, 6–9 November 2005; IEEE: Piscataway, NJ, USA, 2005; p. 6.
150. Bertsimas, D.; Tsitsiklis, J. Simulated annealing. *Stat. Sci.* **1993**, *8*, 10–15. [CrossRef]
151. Goldberg, D.; Sastry, K. *Genetic Algorithms: The Design of Innovation*; Springer: Berlin/Heidelberg, Germany, 2007.
152. Tibshirani, R. Regression shrinkage and selection via the lasso. *J. R. Stat. Soc. Ser. B (Methodol.)* **1996**, *58*, 267–288. [CrossRef]
153. Friedman, J.H. Greedy function approximation: A gradient boosting machine. *Ann. Stat.* **2001**, *29*, 1189–1232. [CrossRef]
154. Meng, L.; Dong, D.; Chen, X.; Fang, M.; Wang, R.; Li, J.; Liu, Z.; Tian, J. 2D and 3D CT radiomic features performance comparison in characterization of gastric cancer: A multi-center study. *IEEE J. Biomed. Health Inform.* **2020**, *25*, 755–763. [CrossRef] [PubMed]
155. Gong, C.S.A.; Su, C.H.S.; Chao, K.W.; Chao, Y.C.; Su, C.K.; Chiu, W.H. Exploiting deep neural network and long short-term memory method-ologies in bioacoustic classification of LPC-based features. *PLoS ONE* **2021**, *16*, e0259140. [CrossRef]
156. Jolliffe, I.T.; Cadima, J. Principal component analysis: A review and recent developments. *Philos. Trans. R. Soc. A Math. Eng. Sci.* **2016**, *374*, 20150202. [CrossRef] [PubMed]
157. Wiltgen, T.; Fleischmann, D.F.; Kaiser, L.; Holzgreve, A.; Corradini, S.; Landry, G.; Ingrisch, M.; Popp, I.; Grosu, A.L.; Unterrainer, M.; et al. 18F-FET PET radiomics-based survival prediction in glioblastoma patients receiving radio (chemo) therapy. *Radiat. Oncol.* **2022**, *17*, 198. [CrossRef]
158. Balakrishnama, S.; Ganapathiraju, A. Linear discriminant analysis—A brief tutorial. *Inst. Signal Inf. Process.* **1998**, *18*, 1–8.
159. Zhao, H.; Wang, Z.; Nie, F. A new formulation of linear discriminant analysis for robust dimensionality reduction. *IEEE Trans. Knowl. Data Eng.* **2018**, *31*, 629–640. [CrossRef]
160. Huang, Y.; Liu, Z.; He, L.; Chen, X.; Pan, D.; Ma, Z.; Liang, C.; Tian, J.; Liang, C. Radiomics Signature: A Potential Biomarker for the Prediction of Disease-Free Survival in Early-Stage (I or II) Non-Small Cell Lung Cancer. *Radiology* **2016**, *281*, 947–957. [CrossRef]
161. Zhao, Z. -Q.; Zheng, P.; Xu, S. -T.; Wu, X. Object Detection With Deep Learning: A Review. *IEEE Trans. Neural Netw. Learn. Syst.* **2019**, *30*, 3212–3232. [CrossRef]
162. Li, C.; Dong, D.; Li, L.; Gong, W.; Li, X.; Bai, Y.; Wang, M.; Hu, Z.; Zha, Y.; Tian, J. Classification of severe and critical covid-19 using deep learning and radiomics. *IEEE J. Biomed. Health Inform.* **2020**, *24*, 3585–3594. [CrossRef] [PubMed]
163. Tomaszewski, M.R.; Gillies, R.J. The biological meaning of radiomic features. *Radiology* **2021**, *298*, 505–516. [CrossRef] [PubMed]
164. Zhang, L.; Wang, M.; Liu, M.; Zhang, D. A Survey on Deep Learning for Neuroimaging-Based Brain Disorder Analysis. *Front. Neurosci.* **2020**, *14*, 779. [CrossRef]
165. Tang, J.; Alelyani, S.; Liu, H. Feature selection for classification: A review. In *Data Classification: Algorithms and Applications*; CRC Press: Boca Raton, FL, USA, 2014; p. 37.
166. Li, J.; Cheng, K.; Wang, S.; Morstatter, F.; Trevino, R.P.; Tang, J.; Liu, H. Feature Selection: A Data Perspective. *ACM Comput. Surv.* **2017**, *50*, 94. [CrossRef]
167. Cai, J.; Luo, J.; Wang, S.; Yang, S. Feature selection in machine learning: A new perspective. *Neurocomputing* **2018**, *300*, 70–79. [CrossRef]
168. Guyon, I.; Gunn, S.; Ben-Hur, A.; Dror, G. Result analysis of the NIPS 2003 feature selection challenge. *Adv. Neural Inf. Process. Syst.* **2004**, *17*. Available online: https://api.semanticscholar.org/CorpusID:2803126 (accessed on 8 August 2023).
169. Porcu, M.; Solinas, C.; Mannelli, L.; Micheletti, G.; Lambertini, M.; Willard-Gallo, K.; Neri, E.; Flanders, A.E.; Saba, L. Radiomics and "radi-… omics" in cancer immunotherapy: A guide for clinicians. *Crit. Rev. Oncol./Hematol.* **2020**, *154*, 103068. [CrossRef]
170. Oliva, J.T.; Lee, H.D.; Spolaôr, N.; Coy, C.S.R.; Wu, F.C. Prototype system for feature extraction, classification and study of medical images. *Expert Syst. Appl.* **2016**, *63*, 267–283. [CrossRef]
171. Park, S.H.; Han, K. Methodologic guide for evaluating clinical performance and effect of artificial intelligence technology for medical diagnosis and prediction. *Radiology* **2018**, *286*, 800–809. [CrossRef] [PubMed]

172. Schwier, M.; Van Griethuysen, J.; Vangel, M.G.; Pieper, S.; Peled, S.; Tempany, C.; Aerts, H.J.; Kikinis, R.; Fennessy, F.M.; Fedorov, A. Repeatability of multiparametric prostate MRI radiomics features. *Sci. Rep.* **2019**, *9*, 9441. [CrossRef]
173. Stanzione, A.; Gambardella, M.; Cuocolo, R.; Ponsiglione, A.; Romeo, V.; Imbriaco, M. Prostate MRI radiomics: A systematic review and radiomic quality score assessment. *Eur. J. Radiol.* **2020**, *129*, 109095. [CrossRef] [PubMed]
174. Ibrahim, A.; Primakov, S.; Beuque, M.; Woodruff, H.; Halilaj, I.; Wu, G.; Refaee, T.; Granzier, R.; Widaatalla, Y.; Hustinx, R.; et al. Radiomics for precision medicine: Current challenges, future prospects, and the proposal of a new framework. *Methods* **2021**, *188*, 20–29. [CrossRef]
175. Dong, D.; He, B.; Kong, B.; Zhang, L.; Tong, L.; Huang, F.; Han, D.; Huang, Z.; Zhang, H.; Tian, J. Abstract CT274: Diagnosis based on signal: The first time break the routinely used circle of signal-to-image-to-diagnose. *Cancer Res.* **2020**, *80*, CT274. [CrossRef]
176. He, B.; Guo, Y.; Zhu, Y.; Tong, L.; Kong, B.; Wang, K.; Sun, C.; Li, H.; Huang, F.; Wu, L.; et al. From signal to knowledge: The diagnostic value of rawdata in artificial intelligence prediction of human data for the first time. *Engineering* **2023**. [CrossRef]